Evaluation of atmospheric gaseous passive samplers through comparison with active *in situ* measurements

CX La Grange

orcid.org 0000-0003-2645-4326

Dissertation accepted in fulfilment of the requirements for the degree *Master of Science in Chemistry* at the North-West University

Supervisor: Prof PG van Zyl
Co-supervisor: Dr K Jaars
Co-supervisor: Dr S Sipahli

Graduation: May 2025

Acknowledgements

Before the onset of my dissertation, I would like to thank a few extraordinary people.

- Firstly, I want to thank my Heavenly Father for giving me the strength and wisdom to further my education.
- To my parents, Peet and Connie la Grange, thank you for your unconditional and unwavering support and love, and for raising me to be a strong and independent individual.
- To my supervisors, Prof Pieter van Zyl, Dr Kerneels Jaars and Dr Shivon Sipahli, thank you for the guidance, knowledge, support and help throughout my studies.
- I express my sincerest gratitude to Johan Prozesky for helping me with the language editing and proofreading of this dissertation.
- To my brother Reyner, as always, thank you for your support and love.
- Finally, to my partner, Johan Pienaar, thank you for your love, understanding and support in my studies.

Abstract

The precise measurement of atmospheric trace gases, including sulphur dioxide (SO_2), nitrogen dioxide (NO_2) and ozone (O_3), is crucial for assessing total changes in the atmosphere that may lead to health complications and exacerbate global warming. The quantification of these species by using passive samplers is a generally acknowledged and frequently utilised method. In some cases, however, it is essential to establish a scaling or correction factor to improve the accuracy and precision of passive samplers in relation to active *in situ* measurements, which are frequently quality checked and calibrated. Scaling factors for certain gaseous species (SO_2 NO_2 and O_3) measured with passive samplers developed and designed by the Atmospheric Chemistry Research Group at the North-West University have previously been calculated. These scaling factors, however, have not undergone evaluation or revision in a considerable amount of time. Therefore, the general aim of this study was to reassess the scaling factors derived from prior research to determine the necessity for adjustments to enhance the precision and accuracy of the passive sampling method. This reassessment was conducted by deploying passive samplers for measurement of atmospheric SO_2 NO_2 and O_3 at Welgegund atmospheric measurement station, which is a comprehensively equipped regional site, between August 2012 and June 2018. Simultaneously, active *in situ* measurement data for these species were measured at Welgegund. The statistical relationships between passive and active *in situ* data were evaluated to validate and amend (if necessary) these scaling factors. This study established the scaling factor for SO_2 at 0.9, formerly calculated as 1.0. The scaling factor for NO_2 found in this study was 1.7, previously recorded as 1.5. The scaling factor for O_3 was established at 1.4 in this study, while the previous scaling factor utilised was 1.3. The scaling factors computed in this investigation are reasonably similar to the previously observed values. However, comprehensive statistical analysis performed in this study showed that it is advisable to update the scaling factors to the newly determined values to enhance the efficacy of the passive sampling approach within the context of the South African environment.

Keywords: Gaseous passive sampler; Scaling factor; Welgegund; Active *in situ* samplers; Inorganic species; DEBITS

Table of Contents

Acknowledgements ..... **i**
Abstract ..... **ii**
Table of Contents ..... **iii**
List of Figures ..... **v**
List of Tables ..... **viii**
1. Introduction **1**
1.1 Background **1**
1.2 Problem Statement **2**
1.3 Objectives **3**
2. Literature Review **2**
2.1 Atmospheric Composition **2**
2.2 Atmospheric Pollution **3**
2.3 Types of Pollution **4**
2.3.1 Particulate Matter 4
2.3.2 Gaseous Species 4
2.4 Impacts of Atmospheric Gaseous Pollutants **5**
2.5 Sources of Inorganic Atmospheric Gaseous Species **6**
2.5.1 Sulphur Species 6
2.5.2 Nitrogen Species 7
2.5.3 Ozone 8
2.6 Transportation, Chemical Transformations and Evolution **9**
2.7 Removal Processes **13**
2.8 Measurement Techniques **14**
2.9 Passive Sampling **14**
2.10 Active sampling techniques **19**
3. Method and Materials **20**
3.1 Site Description **20**
3.2 Reagents and Materials **21**
3.3.1 Passive Sampler Preparation and Assembly 21
3.3.2 Passive Sampling 22
3.3.3 Active *in situ* Measurements 22
3.4 Analysis of Passive Samplers **23**
3.5 Quality Assurance **23**
3.5.1 Passive Samplers and Analytical Technique 23
3.5.2 Active *in situ* Measurements 26
3.6 Data Processing, Statistical Analysis and Calculations **26**
4. Results and Discussion **29**

4.1 Data Availability **29**
4.2 Spearman's Correlations (linear regression) **31**
4.3 Kruskal-Wallis Test **34**
4.4 Bland-Altman Analysis **38**
4.5 Temporal Patterns **44**
4.5.1 Seasonal 44
4.5.2 Inter-Annual 46
5. Conclusion **50**
5.1 Project Evaluation and Main Conclusions **50**
5.1.1 Objective 1 50
5.1.2 Objective 2 51
5.1.3 Objective 3 51
5.1.4 Objective 4 52
5.2 Recommendations and Future Perspectives **52**
References **54**

List of Figures

Figure 2.1 Diagram showing the components (on the left) and assembly (on the right) of a passive sampler. 15

Figure 2.2 The concentration profile outside and inside the passive diffusion sampler showing the thickness of the components. 16

Figure 3.1 Map of the North West province of South Africa with the red star indicating the location of the Welgegund atmospheric monitoring station. A map of South Africa, showing its provinces, is presented at the bottom right. 20

Figure 3.2 The housing unit used for deployment of passive samplers at Welgegund with the aluminium rails in which the passive samplers were placed shown on the right. 22

Figure 3.3 Example of a ring diagram visualising WMO LIS results. 25

Figure 3.4 Results from the WMO LIS 68 study in 2023 for the NWU laboratory. 26

Figure 4.1 Cook's distance calculated for concentrations determined for a) SO_2 b) NO_2 and c) O_3, with passive and active samplers together with the heuristic threshold indicated with a black dotted line. 30

Figure 4.2 Comparison of active in situ measurements with the uncorrected passive measurements for a) SO_2 b) NO_2 and c) O_3 sampled at Welgegund between August 2012 to June 2018. 32

Figure 4.3 A combination of a violin, box and jittered plot of the monthly average SO_2 concentrations determined with the active *in situ* sampler, as well as passive samplers utilising the previously used and new scaling factors determined in this study. Top and bottom line shows the 25^{th} and 75^{th} percentile of concentration, and the middle line and red dot show the median. Whiskers on the boxplots show 95% coverage of the data; the axis is broken along the line to show outliers. The inferential statistics, an estimate of effect size and uncertainty, and pairwise comparisons are also shown. 35

Figure 4.4 A combination of a violin, box and jittered plot of the monthly average NO_2 concentrations determined with the active *in situ* sampler, as well as passive samplers utilising the previously used and new scaling factors determined in this study. Top and bottom line shows the 25^{th} and 75^{th} percentile of concentration, and the middle line and red dot show the median. Whiskers on the boxplots show 95% coverage of the data; the axis is broken along the line to show outliers. The inferential statistics, an estimate of effect size and uncertainty, and pairwise comparisons are also shown. 36

Figure 4.5 A combination of a violin, box and jittered plot of the monthly average O_3 concentrations determined with the active *in situ* sampler, as well as passive samplers utilising the previously used and new scaling factors determined in this study. Top and bottom line shows the 25th and 75th percentile of concentration, and the middle line and red dot show the median. Whiskers on the boxplots show 95% coverage of the data; the axis is broken along the line to show outliers. The inferential statistics, an estimate of effect size and uncertainty, and pairwise comparisons are also shown. 38

Figure 4.6 Similarity of a) accuracy, b) precision, and c) reliability for active *in situ* SO_2 measurements in relation to SO_2 concentrations determined with passive samplers utilising the previously used scaling factor obtained using 5×10^3 bootstrap iterations..... 39

Figure 4.7 Similarity of a) accuracy, b) precision, and c) reliability for active *in situ* SO_2 measurements in relation to SO_2 concentrations determined with passive samplers utilising the new scaling factor obtained using 5×10^3 bootstrap iterations. 39

Figure 4.8 Similarity of a) accuracy, b) precision, and c) reliability for active *in situ* NO_2 measurements in relation to NO_2 concentrations determined with passive samplers utilising the previously used scaling factor obtained using 5×10^3 bootstrap iterations..... 41

Figure 4.9 Similarity of a) accuracy, b) precision, and c) reliability for active *in situ* NO_2 measurements in relation to NO_2 concentrations determined with passive samplers utilising the new scaling factor obtained using 5×10^3 bootstrap iterations. 41

Figure 4.10 Similarity of a) accuracy, b) precision, and c) reliability for active *in situ* O_3 measurements in relation to O_3 concentrations determined with passive samplers utilising the previously used scaling factor obtained using 5×10^3 bootstrap iterations..... 42

Figure 4.11 Similarity of a) accuracy, b) precision, and c) reliability for active *in situ* O_3 measurements in relation to O_3 concentrations determined with passive samplers utilising the new scaling factor obtained using 5×10^3 bootstrap iterations. 43

Figure 4.12 Monthly SO_2 concentrations measured at Welgegund from August 2012 to June 2018 with (a) passive samplers utilising the new scaling factor, and (b) with active *in situ* samplers. The red line of each box represents the median, the top and bottom edges of the box the 25th and 75th percentiles, respectively, the whiskers ±2.7σ (99.3% coverage if the data has a normal distribution) and the black dots the averages. 44

Figure 4.13 Monthly NO_2 concentrations measured at Welgegund from August 2012 to June 2018 with (a) passive samplers utilising the new scaling factor, and (b) with active *in situ* samplers. The red line of each box represents the median, the top and bottom edges of the box the 25th and 75th

percentiles, respectively, the whiskers ±2.7σ (99.3% coverage if the data has a normal distribution) and the black dots the averages. 45

Figure 4.14 Monthly O_3 concentrations measured at Welgegund from August 2012 to June 2018 with (a) passive samplers utilising the new scaling factor, and (b) active *in situ* samplers. The red line of each box represents the median, the top and bottom edges of the box the 25th and 75th percentiles, respectively, the whiskers ±2.7σ (99.3% coverage if the data has a normal distribution) and the black dots the averages. 46

Figure 4.15 Annual SO_2 concentrations measured at Welgegund from August 2012 to June 2018 with (a) passive samplers utilising the new scaling factor, and (b) active *in situ* samplers. The red line of each box represents the median; the top and bottom edges of the box the 25th and 75th percentiles, respectively; the whiskers ±2.7σ (99.3% coverage if the data has a normal distribution); and the black dots the averages. 47

Figure 4.16 Annual NO_2 concentrations measured at Welgegund from August 2012 to June 2018 with (a) passive samplers utilising the new scaling factor, and (b) active *in situ* samplers. The red line of each box represents the median; the top and bottom edges of the box the 25th and 75th percentiles, respectively; the whiskers ±2.7σ (99.3% coverage if the data has a normal distribution); and the black dots the averages. 48

Figure 4.17 Annual O_3 concentrations measured at Welgegund from August 2012 to June 2018 with (a) passive samplers utilising the new scaling factor, and (b) active *in situ* samplers. The red line of each box represents the median; the top and bottom edges of the box the 25th and 75th percentiles, respectively; the whiskers ±2.7σ (99.3% coverage if the data has a normal distribution); and the black dots the averages. 49

List of Tables

Table 2.1 Atmospheric sulphur containing compounds. 6

Table 2.2 Potential atmospheric reactions for ground state SO_2 and SO_3 showing both the enthalpy changes and the rate constants of these reactions. 9

Table 2.3 Diffusion constants for trace gas species. 17

Table 4.1 Data availability for the sampling period after removing outliers and data for months for which no active measurements were conducted. 31

Table 4.2 r_s- and p-values determined from Spearman's correlations between uncorrected passive data and active in situ measurements. 33

Chapter 1

1. INTRODUCTION

This chapter briefly demonstrates why the assessment of ambient inorganic trace species within the atmosphere is important. The discussion of knowledge gaps that follows elucidates the rationale for this study. Thereafter the overarching aim of this study is discussed along with detailed objectives.

1.1 Background

The earth's atmosphere comprises a mixture of gases that forms a thin layer surrounding the globe. The atmosphere is essential for sustaining life as it supplies oxygen and water, while also regulating the surface temperature of the earth (Török and Dransfield, 2018). Gaseous species and/or aerosols emitted into the atmosphere, either naturally or as a result of human activities, are classified as air pollution when atmospheric concentrations of these species accumulate to levels that are detrimental to plants, animals, ecosystems and human health (Monks and Hey, 2009). It is widely recognised that increased anthropogenic activities are changing the chemical composition of the atmosphere (Monks and Hey, 2009). Air pollution in South Africa is exacerbated by rapid population growth and rising energy consumption, which significantly contributes to changes in the chemical composition of the atmosphere (Swartz et al., 2019, Swartz et al., 2020b).

Approximately 90% of the atmospheric mass is located in the troposphere, which extends from the surface of the earth to a height of around 10 to 18 km. The troposphere comprises several trace gas species (Monks and Hey, 2009). The primary means by which gaseous (and particulate) pollutants are introduced into the atmosphere is through the anthropogenic and natural emission of atmospheric trace species into the planetary boundary layer (Seinfeld, 2006). The released trace species are capable of undergoing a wide range of chemical and physical changes after they are emitted into the atmosphere. Changes in the natural concentrations of these species can impact local, regional and global air quality and climate change, especially if the changes are associated with anthropogenic activities (Monks and Hey, 2009). Typical inorganic gaseous pollutants in the atmosphere include sulphur dioxide (SO_2) and nitrogen oxides (NO_x = NO + NO_2), as well as the important secondary pollutant ozone (O_3)(Beukes, 2019).

Concentrations of these species in the atmosphere can be quantified with active *in situ* measurements and/or passive sampling, with the latter being especially useful in remote regions that are logistically difficult to access. The active, continuous or *in situ* measurement technique, uses a variety of photolytic processes, including fluorescence, chemiluminescence, and absorption, to continually monitor trace gas species (Skoog and West, 1963). This approach has greater costs and larger logistical constraints in addition to requiring more complicated measurement techniques (Martins, 2009). This led to the development and deployment of diffusive/passive sampling techniques. Passive sampling has the advantage of being more cost-effective, mobile and easy to

use. At the same time, it does not require regular field calibrations and access to electricity when deployed in the field (Ferm and Rodhe, 1997). There are, however, disadvantages associated with the use of the passive method e.g. specific temporal resolution (averaged concentrations of species over a period of time). Another disadvantage of the diffusion or passive sampler is that this type of sampler can become saturated leading to a rapid decline in sampling efficiency as the adsorbent becomes more saturated (Adley and Underhill, 1989). It is thus important to establish the upper threshold for the exposure time for these types of samplers to prevent the saturation of the sampler (Pienaar et al., 2015). In addition, the passive sampler needs to be regularly evaluated in terms of accuracy and precision through inter-comparison studies, which include comparisons to active *in situ* measurements and other types of passive sampling techniques (Vardoulakis et al., 2009).

In several instances, a scaling or correction factor must be established for these passive samplers in order to improve their accuracy and precision (Vardoulakis et al., 2009). Passive samplers can under- or overestimate the atmospheric levels of gaseous species due to the concentrations of the gaseous species not being directly measured as with an active *in situ* sampler. Gaseous species, for instance, react with a chemical sorbent in the passive sampler that traps the gaseous species of interest, which is then analysed offline. Therefore, as mentioned above, the performance of these passive samplers must be continuously evaluated against active *in situ* measurements.

1.2 Problem Statement

The Atmospheric Chemistry Research Group (ACRG) at the North-West University developed passive samplers based on those developed by the Swedish Environmental Research Institute (IVL) to measure atmospheric concentrations of gaseous species, i.e. sulphur dioxide (SO_2) nitrogen dioxide (NO_2), ozone (O_3), ammonia (NH_3) and nitric acid (HNO_3) at remote South African atmospheric monitoring sites of the Deposition of Biogeochemical Important Trace Species (DEBITS) programme. Comparison of SO_2 NO_2 and O_3 concentrations determined with these passive samplers with active *in situ* measurements by Dhammapala, (1996) indicated that no scaling factor was required for SO_2, while scaling factors of 1.5 and 1.3 were determined for NO_2 and O_3, respectively. Martins, (2009) also reported similar scaling factors for SO_2, NO_2 and O_3. In addition, since no active *in situ* measurements were conducted for NH_3 and HNO_3 in South Africa, a scaling factor of 1 was used for NH_3 and HNO_3, as reported in other studies. Furthermore, the ACRG also participated in an international inter-comparison study of SO_2 and NO_2 passive samplers, in which the passive samplers developed by the ACRG were compared to other passive samplers used in other laboratories, as well as active in situ samplers at the University of Singapore (He and Bala, 2008). This intercomparison study also confirmed good performance of the SO_2 and NO_2 passive samplers used by the ACRG. In this study, SO_2 NO_2 and O_3 passive samplers will be newly evaluated against active *in situ* measurements of these species conducted at a regional atmospheric monitoring site, Welgegund, located in the South African interior.

1.3 Objectives

The general aim of this study was to assess the performance of SO_2, NO_2 and O_3 passive samplers through comparison with active *in situ* measurements of these species conducted at the comprehensively equipped atmospheric measurement station, Welgegund, as well as, if required, to update scaling factors used in the calculations of concentrations of these species determined with passive samplers. Specific objectives included:

- deploying SO_2, NO_2 and O_3 passive samplers for a period of at least 5 years at the Welgegund atmospheric monitoring site;
- processing and analysing active *in situ* measurement datasets determined for these species at Welgegund during the same sampling period;
- determining statistical correlations between passive and active *in situ* measurements, in order to verify and/or establish updated scaling factors to calculate the concentrations of these inorganic gaseous species measured with passive samplers; and
- contextualising and comparing correlations determined in this study with previous comparative studies conducted in South Africa and other parts of the world.

Chapter 2

2. LITERATURE REVIEW

This chapter encompasses a comprehensive literature review for this study. The focus of this review will be on the composition of the atmosphere, along with the sources and impact of atmospheric pollution. Also discussed are the transport, chemical transformation, evolution and removal of inorganic species with a focus on species of sulphur, nitrogen, and ozone. Different sampling techniques for inorganic gaseous species are also described briefly, with the focus on the passive sampling technique.

2.1 Atmospheric Composition

Earth's atmosphere is composed of a mixture of gases that forms a thin layer around the globe. The atmosphere is characterised by a unique composition due to the interaction between biological activity in soils, plants and oceans, and physical and chemical processes in the atmosphere (Monks et al., 2009). The atmosphere plays a crucial role in sustaining life by controlling Earth's surface temperature and serving as a primary supply of oxygen (O_2) and water (H_2O) (Török and Dransfield, 2018). It is hypothesised that the early atmosphere consisted of a combination of gaseous carbon dioxide (CO_2), H_2O, nitrogen (N_2), and small amounts of hydrogen (H_2). However, over time, most of these compounds outgassed (release of a substance as a gas or vapour) and deposited to Earth to form the ocean and carbonate rocks. The atmosphere's composition has shifted from a slightly reduced to a highly oxidised environment (Seinfeld and Pandis, 2006).

The atmosphere comprises two primary layers, i.e. the upper atmosphere and the lower atmosphere (Connell, 2005, Seinfeld and Pandis, 2006), which may further be separated into five layers according to temperature and pressure variations between each layer (Harrison, 1999, Török and Dransfield, 2018). These five atmospheric layers are separated according to the distance from the surface of the earth, which include the troposphere (between the surface of the earth up to 10 to 15 km above the surface, stratosphere (up to 45 to 55 km above the surface), mesosphere (up to 80 to 90 km above the surface), thermosphere (up to 90 to 500 km above the surface), and exosphere (up to 500 km above the surface).

Although the lower layers of the atmosphere near the surface of the earth have a greater impact on life forms, changes in the upper atmosphere may also significantly influence the earth's surface. The rise in temperature, particularly in the twentieth century, has been ascribed to increases in concentrations of greenhouse gases in the upper layers of the atmosphere (Laštovička et al., 2006). The temperature in the troposphere generally decreases with an increase in altitude, with the average rate of temperature decline typically being approximately 9.8 K Km^{-1} (Harrison, 2013). The troposphere, which constitutes 85% to 90% of the total mass of the atmosphere, primarily consists of approximately 78% nitrogen (N_2), 21% oxygen (O_2), 1% argon (Ar), and fewer than 1% trace gases (Brasseur et al., 1999, Seinfeld and Pandis, 2006). The concentrations of these compounds are

controlled by the biosphere, while the release and uptake from crustal material and interior degassing also influence the concentrations of these species (Seinfeld and Pandis, 2006). Additionally, atmospheric H_2O primarily occurs in the troposphere which, together with consistent air turbulence and mixing, give rise to weather and weather-related phenomena (Harrison, 1999). The H_2O vapour content in the atmosphere varies significantly and can account for up to 3% of the total atmospheric composition (Seinfeld and Pandis, 2006). Several important processes occur in the troposphere, including biological activities such as respiration and photosynthesis (Connell, 2005). The troposphere is subdivided into two distinct regions, namely the planetary boundary layer (PBL) that extends from the surface of the earth up to an altitude of approximately 1 km and the free troposphere layer above the PBL (Ritchie, 2017, Seinfeld and Pandis, 2006). The daily maximum average PBL height in South Africa ranges between 1480-2260 m (Korhonen et al., 2014). Most emissions of pollutant species from the earth's surface are limited to the PBL (Seinfeld and Pandis, 2006). However, the free troposphere contains species with longer lifetimes (Harrison, 2013). Contaminants emitted into the troposphere can be trapped in the atmosphere as a consequence of specific meteorological circumstances, leading to the accumulation of pollutant species (Ritchie, 2017). Vertical mixing in the PBL is mainly influenced by atmospheric stability, which is associated with the strength of buoyancy effects (Harrison, 1999). Turbulence is generated by mechanical forces as air flows over irregular landscapes such as hills, buildings, or trees (Harrison, 1999, Seinfeld and Pandis, 2006). Furthermore, vertical movements in the atmosphere, known as up and down currents, are generated by the warming or cooling of the surrounding atmosphere (Seinfeld and Pandis, 2006). When an air mass rises up to the tropopause, which is the boundary between the troposphere and stratosphere, it undergoes a temperature decrease of around 9.7 K km^{-1} (Seinfeld and Pandis, 2006).

2.2 Atmospheric Pollution

Pollution may be defined as a change in the environment due to polluting or unwanted external undesirable substance both from natural and anthropogenic sources (Meetham et al., 2016, Massari et al., 2023). These changes (both chemical and physical) can lead to temporary discomforts as well as permanent damage to living organisms and can generate imbalances within natural cycles. No substance or element can unequivocally be considered a pollutant. The size of the change caused by a certain substance in a specific circumstance can however be seen a polluting (Massari et al., 2023). Air pollutants include both gaseous species and/or aerosols released into the atmosphere by anthropogenic activities or can occur naturally (Seinfeld and Pandis, 2006). These particles can accumulate to sufficiently high levels to cause injury or damage to animals, plants, and ecosystems if not dispersed, diluted or removed from the atmosphere by removal processes (Seinfeld and Pandis, 2006, Monks et al., 2009). It is crucial to acknowledge that anthropogenic activities have caused significant changes in the atmosphere's composition (Brasseur et al., 2006). It is important to distinguish between primary pollutants emitted directly into the atmosphere from sources, and secondary pollutants formed in the atmosphere through chemical reactions and gas-to-particle

transformation (Dieminger et al., 1996, Seinfeld and Pandis, 2006). Pollutants with longer lifetimes can be transported throughout the entire atmosphere, affecting both the lower and upper atmosphere to some extent (Seinfeld and Pandis, 2006). The impacts of air pollution range from local and regional to global scales (Finlayson-Pitts and Pitts, 1997). Atmospheric pollutants are composed of particulate matter (PM) and gaseous species (Petäjä et al., 2013).

2.3 Types of Pollution

2.3.1 Particulate Matter

PM or aerosols are liquid or solid species suspended in the atmosphere with sizes ranging from 10^{-9} to 10^{-4} m (Pöschl, 2005, Monks et al., 2009, Manisalidis et al., 2020). Typical natural sources of aerosols include naturally occurring biomass burning, volcanic eruptions, and biological materials while anthropogenic sources include fossil fuel combustion along with biomass burning for domestic heating (Seinfeld and Pandis, 2006). Atmospheric PM undergoes several chemical and physical interactions and transformations, including changes in their dimensions (size) and chemical composition (Pöschl, 2005).

2.3.2 Gaseous Species

Pollutant gaseous species in the atmosphere occur in relatively small (trace) amounts in the atmosphere, i.e. approximately 1% of the atmosphere's composition. However, these species contribute significantly to changes in the atmosphere (Seinfeld and Pandis, 2006) with small increases in emissions of these species substantially impacting the atmosphere and associated chemistry (Monks and Hey, 2009). Atmospheric gaseous species include organic and inorganic species.

2.3.2.1 Volatile Organic Compounds

Volatile organic compounds (VOCs) are gaseous organic species that are directly emitted from both biogenic and anthropogenic sources (Mozaffar and Zhang, 2020) or can form in the atmosphere as secondary pollutants. These VOCs mostly are composed of aromatic hydrocarbons, such as toluene and benzene, but exclude both carbon monoxide (CO) and carbon dioxide (CO_2) (Atkinson, 2000, Seinfeld and Pandis, 2006). Anthropogenic VOCs originate from several sources such as petrochemical processes, combustion processes, automobile emissions, fuel storage and transportation, solvent usage and production, as well as hazardous waste sites and landfills (Jaars et al., 2014). During the dry season in southern Africa, veld fires (open biomass burning) can release large amounts of VOCs (Jaars et al., 2014). VOCs are involved in chemical and photochemical reactions that result in the production of tropospheric O_3 and secondary organic aerosols (SOA) (Jaars et al., 2014) with VOCs being one of the most important precursor species for the formation of these secondary pollutants (Chen et al., 2022).

2.3.2.3 Inorganic Compounds

In the pursuit of understanding air pollution and assessing air quality, inorganic gaseous pollutants play a substantial role (Seigneur, 2019). These compounds can in heightened concentrations be harmful to the environment in several ways. These species play a crucial role in the chemical processes occurring in the atmosphere with some of these species being highly reactive. Typical inorganic gaseous species occurring in the atmosphere include carbon oxide (CO_x), nitrogen oxide and -dioxide (NO and NO_2), sulphur dioxide (SO_2), ammonia (NH_3), nitric acid (HNO_3),and O_3 (Martins, 2009, Liu et al., 2021). In the last century, there has been a notable rise in the global levels of these inorganic gaseous species due to a substantial increase in emissions caused by human activity (Martins, 2009, Meng et al., 2009).

2.4 Impacts of Atmospheric Gaseous Pollutants

Pollution has far-reaching impacts on the environment and health, which include air quality and climate change. The level of environmental pollution has escalated to a degree that presents a significant hazard to human health, wildlife, and vegetation (Najjar, 2011). Furthermore, impacts on the ecological systems include lake acidification, coastal water eutrophication, and mercury bioaccumulation in aquatic food webs (Lovett et al., 2009). Pollutants can exert either a net cooling or warming influence on the atmosphere (Scholes et al., 1996) with greenhouse gases, such as CO_2 O_3, and CH_4 contributing to global warming (Jeffry et al., 2021). Climate change is considered a significant event in terms of air pollution since it has ecological, political, economic, and social implications (Scholes et al., 1996). Pollutants can directly affect human health by entering the respiratory system or bloodstream, leading to various health issues (Scholes et al., 1996, Jion et al., 2023). Tropospheric O_3 is harmful when found in excessive amounts at ground level, since it negatively impacts cardiovascular and respiratory systems (Connell, 2005). The depletion of O_3, on the other hand, might result in heightened exposure to radiation, hence increasing the susceptibility of individuals to develop skin cancer (Connell, 2005). O_3 can cause substantial damage to plants, due to its severe phytotoxicity. The phytotoxicity effect of O_3 can weaken or damage plants and impede photosynthesis (Blum and Didyk, 2007). When O_3 enters a solution it can decompose into several chemical components, including free radicals of hydroxyl and organic origin, superoxide anions as well as hydrogen peroxide, attacking several biochemical sites on a plant (Pell, 1987). In addition, SO_2, NO_x (NO_x = NO + NO_2) and VOCs are considered to be harmful air pollutants for humans (Jion et al., 2023). Inhaling high levels of CO can lead to immediate poisoning, while elevated levels of NO_2 have detrimental effects on plants and can negatively impact agricultural productivity. Additionally, NO_2 emissions contribute to both global warming and eutrophication (Barker and Tingey, 2012, Jion et al., 2023). SO_2 is associated with acid rain, ozone depletion, respiratory conditions, eutrophication, and contributions to global warming (Chen et al., 2007, Niu et al., 2011, Slezakova et al., 2011, Su et al., 2013, Hao et al., 2018, Wang et al., 2021, Jion et al.,

2023). It has also been noted that prolonged exposure to both SO_2 and NO_2 can respectively result in chronic bronchitis and pulmonary asthma (Lourens et al., 2011).

2.5 Sources of Inorganic Atmospheric Gaseous Species

Atmospheric sulphur- and nitrogen species, as well as O_3 are further explored in terms sources, transportation, chemical transformation, evolution and removal processes, with a specific focus SO_2, NO_2 and O_3 as these species are measured in this study. SO_2, NO_2 and O_3 are considered significant air pollutants based on their impacts briefly discussed in **Section 2.4** (Üzmez, 2018). SO_2 and NO_2 are typical major air pollutants that are found in significant quantities in areas with extensive industrial operations (Bozkurt et al., 2018, Jion et al., 2023). O_3 is a secondary pollutant that is created in the troposphere by photochemical reactions involving NO_x and VOCs, as previously described (Bozkurt et al., 2015).

2.5.1 Sulphur Species

The concentration of sulphur in the crust of the earth is below 500 ppm by mass, while the concentration of sulphur in the atmosphere is below 1 ppm in terms of total volume mixing (Seinfeld and Pandis, 2006). Nevertheless, compounds that include sulphur have a substantial influence on both the temperature and the chemistry of the atmosphere. Table 2.1, adapted from Seinfeld and Pandis (2006), displays the many compounds that include sulphur found in the environment. The primary sulphur compounds present in the atmosphere include SO_2, CS_2, OCS, CH_3SCH_3, and H_2S (Seinfeld and Pandis, 2006).

Table 2.1 Atmospheric sulphur containing compounds.

Compound		Most prevalent atmospheric state
Name	**Formula**	
Hydrogen sulphide*	H_2S	Gas
Dimethyl sulphide (DMS)	CH_3SCH_3	Gas
Carbon disulphide	CS_2	Gas
Carbonyl sulphide	OCS	Gas
Methyl mercaptan	CH_3SH	Gas
Dimethyl disulphide	CH_3SSCH_3	Gas
Dimethyl sulphoxide	CH_3SOCH_3	Gas
Sulphur dioxide*	SO_2 or $SO_2 \cdot H_2O$	Gas/Aqueous
Bisulphite ion*	HSO_3^-	Aqueous

Sulphite ion*	SO_3^{2-}	Aqueous
Sulphuric acid*	H_2SO_4	Gas aqueous/aerosol
Bisulphate ion*	HSO_4^-	Aqueous/aerosol
Sulphate ion*	SO_4^{2-}	
Methane sulphonic acid (MSA)	CH_3SO_3H	Gas/Aqueous
Dimethyl sulphone	$CH_3SO_2CH_3$	Gas
Hydroxy methane sulphonic acid (HMSA)	$HOCH_2SO_3H$	Aqueous

*Inorganic sulphur species

Fossil fuel combustion, pyrometallurgical and industrial operations, electricity generation, vehicle emissions, and biomass burning (wildfires and home combustion) are the primary anthropogenic sources of atmospheric SO_2 (Fields, 2004, Josipovic et al., 2011, Zheng et al., 2018, Jion et al., 2023). Volcanoes and the decomposition of organic matter from both plants and animals are two natural sources of sulphurous gases (Jion et al., 2023). Volcanic eruptions emit large amounts of SO_2 and other sulphurous chemicals, such as H_2S, coupled with nitrogen compounds and other aerosols (Monroe et al., 2006, Seinfeld and Pandis, 2006, Zheng et al., 2018). In addition to volcanic eruptions, biomass burning, aquatic habitats, including oceans and wetlands, soils and plants produce H_2S into the atmosphere (Seinfeld and Pandis, 2006). Most CH_3SCH_3 (DMS) come from aquatic biological activity and photochemical processes (Ayres et al., 1997, Seinfeld and Pandis, 2006). While OCS and CS_2 fluxes are minor relative to overall sulphur emissions, they should nevertheless be included in atmospheric chemistry (Lee and Brimblecombe, 2016). These chemicals have several sources that overlap with other sulphur-containing compounds. OCS and CS_2 come from biomass burning, biofuel combustion, industrial activity (paper and pulp, rayon/cellulosic, pigment, food processing, gas, metal and brick making), vehicle emissions, landfills, and oxidation (Lee and Brimblecombe, 2016).

2.5.2 Nitrogen Species

Nitrogen is essential to the environment and all living things (Seinfeld and Pandis, 2006). It makes up 78% of Earth's atmosphere (Fields, 2004, Seinfeld and Pandis, 2006). Not all types of nitrogen are reactive because N_2 molecules have strong bonds, preventing them from playing a significant role in the environment (Fields, 2004, Seinfeld and Pandis, 2006). The atmosphere's main nitrogen compounds include NO_2, NO, N_2O, NH_3 and HNO_3 (Seinfeld and Pandis, 2006). The nitrogen oxides NO and NO_2 known as NO_x are important atmospheric compounds (Seinfeld and Pandis, 2006). The combustion of fossil fuels including coal, natural gas, and fuel oil and emissions from automobile exhausts, power production, and biomass burning (for heating and cooking) are the main sources of atmospheric NO_x (Bozkurt et al., 2015, Jion et al., 2023). It is generally assumed that fossil fuels

produce 50% of atmospheric NO_x (Fields, 2004, Josipovic et al., 2011). Human activities increase NO_2 production by making fertilisers using the Haber-Bosch process (Zbieranowski and Aherne, 2012). However, lightning, biomass burning like veld fires, and soil emissions also release NO_x (Fields, 2004, Seinfeld and Pandis, 2006). Other nitrogen species may be present in the atmosphere due to NO_x surface-atmosphere interactions. Mostly responsible for producing reactive nitrogen species in the stratosphere is nitrous oxide (N_2O), a powerful greenhouse gas. These species are essential for catalytic O_3 depletion. N_2O is emitted by agricultural soils, oceans, animal waste, biomass burning, fuel combustion, and industrial operations, with nitrogen-based fertiliser being the main source (Stein and Yung, 2003, Seinfeld and Pandis, 2006). NH_3 is the third most abundant nitrogen component within the atmosphere with natural sources ranging from crops, animals, soil and the ocean, while biomass burning, synthetic fertilisers and industrial operations are anthropogenic sources (Seinfeld and Pandis, 2006). Additional minor atmospheric nitrogen compounds include reactive nitrogen species (NO_y), which includes NO_x and all other byproducts of atmospheric NO_x oxidation (Seinfeld and Pandis, 2006). According to Seinfeld and Pandis (2006), these NO_y species mentioned include nitric acid (HNO_3), dinitrogen pentoxide (N_2O_5), the nitrate radical ($NO_3^{\cdot}$), peroxynitric acid (HNO_4), peroxyalkyl nitrates ($ROONO_2$), nitrous acid (HONO), peroxyacetyl nitrate (PAN) ($C_2H_3NO_5$), and its homologs and alkyl nitrates ($RONO_2$) (Seinfeld and Pandis, 2006). Many biological and abiotic processes that generate and consume NO_y affect soil surface NO_y emissions where nitrification and denitrification are the major sources of NO_y (Fowler et al., 2009). The only two known ways of producing HNO_3 in the atmosphere are the chemical reaction between NO_x and $HO^{\cdot}$ radicals, or the heterogeneous conversion of N_2O (Brasseur et al., 1999, Fields, 2004). HNO_3 is the primary oxidation product of NO_x in the environment. Its high water solubility causes it to settle quickly on surfaces and in H_2O droplets (Seinfeld and Pandis, 2006).

2.5.3 Ozone

The earth's atmosphere produces modest quantities of reactive oxidant gas O_3 (Seinfeld and Pandis, 2006). As shown in **Chapter 2** in **Sections 2.1** and **Section 2.4**, stratospheric O_3 is crucial. Suitable upper troposphere and lower stratosphere conditions can discharge O_3 into the troposphere (Connell, 2005). Photochemical processes involving natural organic chemicals, nitrogen oxides, and stratospheric contributions increase O_3 (Finlayson-Pitts and Pitts, 1997). The primary anthropogenic origin of O_3 in photochemical smog is the process of NO_2 being broken down by sunshine or UV radiation, known as photodissociation. O_3 is produced as a secondary pollutant when nitrogen oxides (NO_x) combine with VOCs in the presence of heat and sunshine (Finlayson-Pitts and Pitts, 1997, Abiodun et al., 2014). Furthermore, research has indicated that halogen species have the potential to enhance the production of atmospheric O_3 when VOCs and NO_x are present (Tanaka et al., 2000).

2.6 Transportation, Chemical Transformations and Evolution

The transport of gaseous species in the atmosphere is influenced by a multitude of favourable meteorological mechanisms, making it vital to understanding pollution spread (Connell, 2005, Swartz, 2016). Solar radiation and Earth's rotation carry pollutants through the atmosphere. Due to the sun's angle, solar energy fluctuates with latitude, making the equator warmer and the poles colder (Harrison, 1999). At the equator, there is a convergence of cold air from the north and south, while warm air ascends. When warm air migrates towards the poles and sinks into their frigid regions, a comparable situation occurs there. The Coriolis force, which arises from the rotation of Earth, exerts a key influence on circulation patterns. For example, air moving in a southern direction towards the equator seems to be influenced by a westward force (Harrison, 1999). The distribution of temperature and patterns of circulation are affected by the proportions of incoming energy that are reflected, absorbed, and re-emitted at a longer wavelength. The ratios vary based on the locale. The processes of H_2O evaporation, cloud formation, and precipitation have a significant influence on circulation patterns and the balance of energy (Harrison, 1999). Various chemical and physical reactions occur in the atmosphere, leading to changes in the oxidised forms or physical properties of gaseous species, alongside their circulation.

Examining the chemical changes and interactions of compounds containing sulphur in the atmosphere, it is seen that, SO_2 when generated by the sources described in **Section 2.5.1**, undergoes oxidation in the atmosphere. Plumes involving the oxidation of sulphur dioxide can undergo two distinct processes (Seinfeld and Pandis, 2006). The routes involved in this process consist of the gas-phase pathway, which is driven by hydroxyl radicals ($OH^{\cdot}$), and the liquid-phase oxidations that occur either with O_3 near a neutral liquid or with hydrogen peroxide (H_2O_2)in a more acidic environment (Seinfeld and Pandis, 2006). **Table 2.2** (Calvert et al., 1978, Hewitt, 2001) displays all the gas-phase reactions and variations of SO_2 that are thermodynamically feasible in the lower atmosphere.

Table 2.2 Potential atmospheric reactions for ground state SO_2 and SO_3 showing both the enthalpy changes and the rate constants of these reactions.

Reaction	Enthalpy change $-\Delta H^{\circ}$ (kJ mol^{-1}) at 25°C	Rate constant (cm^3 mol^{-1} s^{-1})
$O_2(\,^1\Delta_g) + SO_2 \rightarrow SO_4$ (biradical)	105	3.9×10^{-20}
$O_2(\,^1\Delta_g) + SO_2 \rightarrow SO_4$ (cyclic)	~117	3.9×10^{-20}
$O_2(\,^1\Delta_g) + SO_2 \rightarrow SO_3 + O(\,^3P)$	-56.5	3.9×10^{-20}
$O_2(\,^1\Delta_g) + SO_2 \rightarrow O_2\left(\,^3\sum_g^-\right) + SO_2$	94	3.9×10^{-20}

$O_2(\,^1\sum_g^+) + SO_2 \rightarrow SO_4$ (biradical)	167	6.6×10^{-16}
$O_2(\,^1\sum_g^+) + SO_2 \rightarrow SO_4$ (cyclic)	180	6.6×10^{-16}
$O_2(\,^1\sum_g^+) + SO_2 \rightarrow SO_3 + O(\,^3P)$	6.3	6.6×10^{-16}
$O_2(\,^1\sum_g^+) + SO_2 \rightarrow SO_2 + O_2(\,^1\Delta_g)$	62.8	6.6×10^{-16}
$O(\,^3P) + SO_2(+M) \rightarrow SO_3(+M)$	347	5.7×10^{-14}
$O_3 + SO_2 \rightarrow O_2 + SO_3$	241	$< 8 \times 10^{-24}$
$NO_2 + SO_2 \rightarrow NO + SO_3$	41.4	8.8×10^{-30}
$NO_3 + SO_2 \rightarrow NO_2 + SO_3$	136	$< 7 \times 10^{-21}$
$ONOO + SO_2 \rightarrow NO_2 + SO_3$	~126	$< 7 \times 10^{-21}$
$N_2O_5 + SO_2 \rightarrow N_2O_4 + SO_3$	100	$< 4 \times 10^{-23}$
$HO_2 + SO_2 \rightarrow HO + SO_3$	69.9	$< 8.7 \times 10^{-16}$
$HO_2 + SO_2(+M) \rightarrow HO_2SO_2(+M)$	29.3	$< 8.7 \times 10^{-16}$
$CH_3O_2 + SO_2 \rightarrow CHO_3O + SO_3$	~113	$< 5.3 \times 10^{-15}$
$CH_3O_2 + SO_2(+M) \rightarrow CHO_3O_2SO_2(+M)$	~130	$< 5.3 \times 10^{-15}$
$(CH_3)_3CO_2 + SO_2 \rightarrow (CH_3)_3CO + SO_3$	~109	$< 7.3 \times 10^{-19}$
$(CH_3)_3CO_2 + SO_2 \rightarrow (CH_3)_3CO_2SO_2$	~126	$< 7.3 \times 10^{-19}$
$CH_3COO_2 + SO_2 \rightarrow CH_3CO_2 + SO_3$	~138	$< 1.3 \times 10^{-18}$
$CH_3COO_2 + SO_2 \rightarrow CH_3COO_2SO_2$	~155	$< 1.3 \times 10^{-18}$
$HO + SO_2(+M) \rightarrow HOSO_2(+M)$	~155	1.1×10^{-12}
$CH_3O + SO_2(+M) \rightarrow CH_3OSO_2(+M)$	~100	$\sim 6 \times 10^{-15}$
$SO_3 + H_2O \rightarrow H_2SO_4$	24.8	9.1×10^{-13}

However, the oxidation processes for SO_2 in **Table 2.2** are limited due to the varying quantities in the atmosphere and their corresponding rate constants (Hewitt, 2001). Therefore, particular attention may be given to the reactions outlined in **Equations 2.1 to 2.4**, which occur in the atmosphere (Seinfeld and Pandis, 2006). The interaction of SO_2 with oxygen (O_2) to form SO_3 is thermodynamically favourable. This reaction is represented by **Equation 2.1** (Seinfeld and Pandis,

2006, Martins, 2009). The SO_2 molecule combines with the $OH^{\cdot}$ to generate hydroxy sulphonyl ($HOSO_2$), represented by **Equation 2.2** with M representing either N_2 or O_2 (Connell, 2005, Seinfeld and Pandis, 2006, Swartz, 2016).

$$2SO_2 + O_2 \rightarrow 2SO_3 \quad (2.1)$$

$$SO_2 + OH\cdot + M \rightarrow HOSO_2\cdot + M \quad (2.2)$$

The $HOSO_2$ radical intermediate reacts with O_2 to form SO_3 and an $OH^{\cdot}$ radical as shown in **Equation 2.3** (Atkinson, 2000, Seinfeld and Pandis, 2006, Swartz, 2016).

$$HOSO_2\cdot + O_2 \rightarrow HO_2\cdot + SO_3 \quad (2.3)$$

The SO_3 formed, in turn forms sulphuric acid (H_2SO_4) through **Equation 2.4**. The oxidation of sulphur dioxide is strongly influenced by humidity with little oxidation taking place in relative humidity below 70% (Connell, 2005, Seinfeld and Pandis, 2006).

$$SO_3 + H_2O + M \rightarrow H_2SO_4 + M \quad (2.4)$$

Equation 2.5 shows the overall reaction of SO_2 in the presence of moisture (H_2O) and O_2 produce H_2SO_4 (Connell, 2005).

$$2SO_2 + H_2O + O_2 \rightarrow 2H_2SO_4 \quad (2.5)$$

The liquid-phase oxidation is another medium for oxidation. SO_2 has the ability to dissolve in H_2O droplets and reach a state of equilibrium as dictated by Henry's law constant (Hewitt, 2001). Due to this, dissolved SO_2 can exist in three distinct forms within a H_2O medium: hydrated SO_2, represented by **Equation 2.6**, bisulphite ions (HSO_3^-), represented by **Equation 2.7**, and sulphite ions (SO_3^{2-}), represented by **Equation 2.8** (Hewitt, 2001, Seinfeld and Pandis, 2006). The prevailing form, however, is contingent upon the acidity of the solution, as the equilibrium is determined by the concentration of hydrogen (Hewitt, 2001). The prevalent form in neutral to slightly acidic conditions (pH of around 7) will predominantly produce hydrated SO_2 while moderately acidic conditions (pH 4-6) show the bisulphite ion as the prevalent for, in highly acidic conditions (pH of 4 and lower) the prevalent form will be the sulphite ion (Martin and Damschen, 1981).

$$SO_2 + H_2O \rightleftharpoons SO_2\cdot H_2O \quad (2.6)$$

$$SO_2\cdot H_2O \rightleftharpoons HSO_3^- + H^+ \quad (2.7)$$

$$HSO_3^- \rightleftharpoons SO_3^{2-} + H^+ \quad (2.8)$$

As stated in **Section 2.5.2**, N_2 is not chemically reactive and must undergo a process termed nitrogen fixation in order to become more reactive and have a significant impact on the environment (Seinfeld and Pandis, 2006). The sources of nitrogen fixation are responsible for the production of NO_y

species. NO_2 is formed as a byproduct when NO is oxidised in the atmosphere, as demonstrated by **Equation 2.9** (Connell, 2005, Seinfeld and Pandis, 2006, Swartz, 2016).

$$2NO + O_2 \rightarrow 2NO_2 \quad (2.9)$$

The oxidation of NO_2 within the atmosphere gives way to the formation of NO_3 radicals (**Equation 2.10**) (Finlayson-Pitts and Pitts Jr, 1993, Connell, 2005).

$$NO_2 + O_3 \rightarrow NO_3^{\cdot} + O_2 \quad (2.10)$$

These radicals undergo decomposition throughout the day (and to a lesser extent at night) through two distinct routes as seen in **Equation 2.11** and **Equation 2.12,** and the trajectory taken is dictated by the wavelength of the radiation that propels the reaction (Connell, 2005, Seinfeld and Pandis, 2006).

$$NO_3^{\cdot} \xrightarrow{h\nu} NO^{\cdot} + O_2 \quad (2.11)$$

$$NO_3^{\cdot} \xrightarrow{h\nu} NO_2 + O^{\cdot} \quad (2.12)$$

During nighttime, the development of radicals occurs. The $NO_3^{\cdot}$ have the ability to react with NO_x (both NO and NO_2), leading to the production of either additional NO_2 (**Equation 2.13**) or the creation of N_2O_5 (**Equation 2.14**) (Connell, 2005, Swartz, 2016).

$$NO_3^{\cdot} + NO \rightarrow 2NO_2 \quad (2.13)$$

$$NO_3^{\cdot} + NO_2 \rightarrow N_2O_5 \quad (2.14)$$

The N_2O_5 formed now reacts in the presence of H_2O, to form HNO_3 shown by **Equation 2.15** (Finlayson-Pitts and Pitts Jr, 1993, Connell, 2005).

$$N_2O_5 + H_2O \rightarrow 2HNO_3 \quad (2.15)$$

Ozone production in the troposphere requires NO_2 photodissociation; this is the only known mechanism for O_3 production in this region (Finlayson-Pitts and Pitts Jr, 1993, Connell, 2005). This process occurs in two distinct processes. The first step involves the photolysis of NO_2, as represented by **Equation 2.16**. The second step involves the creation of O_3 in the presence of either N_2 or O_2, as shown by the symbol M in **Equation 2.17** (Finlayson-Pitts and Pitts Jr, 1993, Connell, 2005).

$$NO_2 \xrightarrow{h\nu} NO + O \quad (2.16)$$

$$O + O_2 + M \rightarrow O_3 + M \quad (2.17)$$

O_3 photolysis results in the generation of the $OH^{\cdot}$, which play a significant role in the atmosphere. The mechanism to produce $OH^{\cdot}$ start with O_3 undergoes photolysis, which produces an excited oxygen atom denoted by an asterisk in **Equation 2.18**. This excited oxygen atom then reacts with H_2O to generate the $OH^{\cdot}$, as illustrated in **Equation 2.19** (Finlayson-Pitts and Pitts Jr, 1993, Connell, 2005, Swartz, 2016).

$$O_3 \xrightarrow{hv} O^* + O_2 \quad (2.18)$$

$$O^* + H_2O \rightarrow 2OH^{\cdot} \quad (2.19)$$

2.7 Removal Processes

Sink processes, also known as removal processes, encompass both natural and anthropogenic mechanisms that eliminate gaseous species from the atmosphere, hence reducing the potential influence of these species on the atmosphere. Sinks can also be regarded as mechanisms that remove gaseous species, resulting in negative emissions (Holmberg et al., 2021).

The main processes by which atmospheric substances are eliminated from the atmosphere include dry- and wet-deposition, as well as chemical changes, as mentioned in this chapter in **Section 2.6** (Josipovic et al., 2011). Wet deposition and dry deposition mechanisms supply vital nutrients to ecosystems (Waldman et al., 1992, Seinfeld and Pandis, 2006). Wet deposition is controlled by precipitation mechanisms and encompasses all processes in which airborne substances are deposited onto the earth's surface in a liquid form. Wet deposition can be categorised into two processes: in-cloud scavenging or rainout, and the collection of hydrometeors such as snowflakes, raindrops, or fog droplets (Kajino and Aikawa, 2015). The chemical composition of these precipitation events reflects the complex interaction of physical and chemical mechanisms within the atmosphere. Wet deposition occurs through three distinct mechanisms: the collision of atmospheric particles with droplets within and below clouds; the use of atmospheric particles as nuclei for the condensation of atmospheric H_2O; and the dissolution of atmospheric gases in airborne droplets (Seinfeld and Pandis, 2006). Dry deposition refers to the direct transfer of both gaseous and particulate species to the earth's surface without the assistance of precipitation (Seinfeld and Pandis, 2006). The process of dry deposition of pollutant species is affected by air turbulence, the characteristics of the surface, and the chemical properties of the gaseous species (Seinfeld and Pandis, 2006, Swartz, 2016).

The elimination and absorption of SO_2 from the atmosphere are controlled by chemical interactions between SO_2 and other molecules in the atmosphere, as well as by dry deposition and the movement of air out of the urban airshed (Seinfeld and Pandis, 2006). **Equation 2.20** illustrates the primary process by which NO_x is removed from the atmosphere during the day with M representing a collision partner (Amedro et al., 2020). However, throughout the night, NO_2 does not undergo photolysis, leading to a completely different chemical behaviour within the NO_x family. Any NO that is present during nighttime has a fast reaction with O_3 as shown in **Equation 2.21** (Seinfeld and Pandis, 2006).

The oxidation of atmospheric NO_x, which leads to the creation of HNO_3, is easily deposited by wet deposition due to its high H_2O solubility (Fields, 2004).

$$OH + NO_2 + M \rightarrow HNO_3 + M \quad (2.20)$$

$$NO_2 + O_3 \rightarrow NO_3^{\cdot} + O_2 \quad (2.21)$$

Both dry deposition and *in situ* chemical loss are the main ways in which O_3 is removed from the atmosphere, as *in situ* chemical synthesis and consumption play a major role in determining the levels of tropospheric O_3. The concentration of NO plays a crucial role in deciding whether the atmosphere in a certain area acts as a source or a sink for O_3 (Seinfeld and Pandis, 2006).

2.8 Measurement Techniques

There are two commonly used techniques for measuring the gaseous contaminants in the atmosphere. The monitoring of inorganic gaseous species with both *in situ* active techniques and passive samplers is well-established in South Africa (Lourens et al., 2011)**.** The first technique, known as *in situ* active sampling, employs several photolytic processes such as absorption, chemiluminescence, and fluorescence to continually monitor trace gas species (Skoog and West, 1963, Martins, 2009). Annular denuders and non-dispersive infrared gas analysers (NDIR) are occasionally employed as supplementary active methods. This way of taking measurements, albeit more advanced, is accompanied by increased costs and additional logistical constraints (Martins, 2009). Consequently, the diffusive or passive technique was devised. This technique has been employed for a considerable period of time with notable achievements (Namiesnik et al., 1984). The primary benefits of this sampling approach are its cost-effectiveness and convenience of handling during the whole sampling process. This type of sampling also has the advantage of being easily transportable and not necessitating on-site electrical calibrations (Ferm and Rodhe, 1997, Üzmez, 2018). However, there are some disadvantages associated with this method, namely in relation to resolution, accuracy, and precision (Vardoulakis et al., 2009). Passive samplers may inaccurately estimate air levels of gaseous species, either by underestimating or overestimating, because they do not immediately monitor the concentrations of these species in real time like an *in situ* active sampler does (Martins, 2009). Passive sampling techniques are further discussed below, since the primary aim of this study was the evaluation of passive samplers used to measure SO_2, NO_2 and O_3.

2.9 Passive Sampling

The passive sampling approach, also known as the diffusive sampling technique, is considered a practical alternative to *in situ* active sampling. This methodology offers the advantage of being easy to use, and being significantly more cost-effective compared to the active sample method. The method of measuring gaseous species has a well-established track record and a long history of being utilised for this specific purpose (Namiesnik et al., 1984, Swartz, 2016). The European

Committee for Standardisation has defined a diffusive sampler as a device that can collect samples of gases or vapours from the atmosphere. The sampling rate is controlled by a physical process, such as gaseous diffusion through a static air layer or a porous material, or permeation through a membrane. However, the device does not involve the active movement of air (Carmichael et al., 2003). The quantification of both SO_2 and NO_2 using diffusive passive samplers is founded on the research conducted by Ferm (1991). Similarly, the measurement of O_3 utilising passive samplers is built upon the work of Koutrakis (1993) and has been widely employed in several studies since. The Atmospheric Chemistry Research Group (ACRG) at the North-West University developed passive samplers based on the Swedish Environmental Research Institute (IVL) passive samplers. This diffusive passive sampler is composed of many components, and it utilises a filter (25 mm) impregnated with a sorbent specifically developed to capture the specific gaseous species of interest. The passive sampler housing comprises a sample cup containing the impregnated filter, a support ring that holds the sample cup and top assembly together, and the top assembly itself, which includes a Teflon filter, a stainless-steel mesh plate, and a top cap with a hole. The configuration of the passive sampler is depicted in **Figure 2.1** (Ferm, 1991, Martins, 2009, Adon et al., 2010, Swartz, 2016).

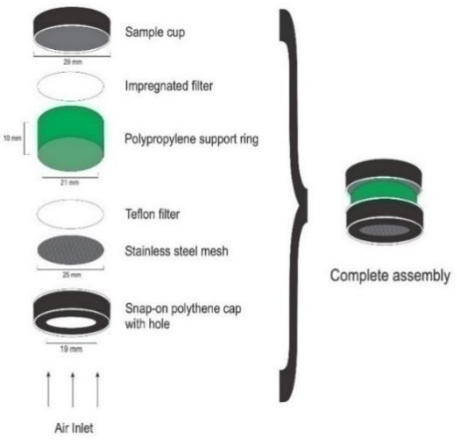

Figure 2.1 Diagram showing the components (on the left) and assembly (on the right) of a passive sampler.

This sampler is suitable for capturing any gas retained on a filter without any leakage to the walls or inlets (Ferm, 1991). The operation of this sampler is based on the passive transport of gas to the sorbent-filled filter through molecular diffusion and chemical reactions with the absorbing solution. The diffusion rate is kept constant by placing the impregnated filter inside a casing (Ferm, 1991, Swartz, 2016). The rate of diffusion is determined by the diffusion constants of each gas, as described by Fick's law (Ferm, 1991, Carmichael et al., 2003, Martins, 2009, Swartz, 2016). The interaction between the trace gas and the solution that absorbs it results in a concentration gradient and a net flux (resulting from the atmosphere and the surface of the material that absorbs it) (Carmichael et al., 2003, Swartz, 2016). **Figure 2.2** illustrates the concentration distribution of a gaseous pollutant within and outside the sampler, as well as the path taken by the pollutant gas

molecules from the entrance to the impregnated filter at the back of the sampler (Ferm, 1991, Dhammapala, 1996, Martins, 2009, Swartz, 2016).

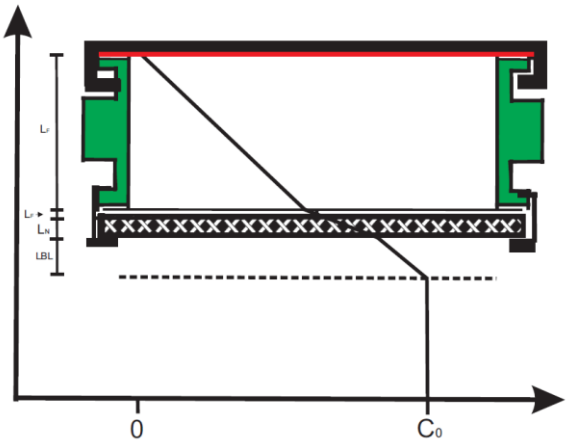

Figure 2.2 The concentration profile outside and inside the passive diffusion sampler showing the thickness of the components.

Figure 2.2 displays the thickness of the plastic ring (L_R), the thickness of the PTFE filter pores (L_F), the thickness of the steel mesh (L_N), and the thickness of the static layer (L_S). In order to determine the concentrations of gaseous species from the passive sampler, Fick's law of diffusion is employed to compute the net flow Φ (μg m^{-2} s^{-1}). The net flow is directly proportional to the concentration gradient C (μg m^{-3}) along the route length L (m) within the sampler, as demonstrated by **Equation 2.25** (Ferm, 2001, Martins, 2009, Swartz, 2016). Where the net flux is represented by Φ (μg m^{-2} s^{-1}), D (m^2 s^{-1}) represents the diffusion coefficient of the gaseous species, and $-\frac{dC}{dL}$ represents the instantaneous concentration gradient of pollutant in the direction of airflow.

$$\Phi = -D\frac{dC}{dL} \tag{2.25}$$

In addition, since passive sampling is time-integrated, the net flow may be determined using **Equation 2.26**. This equation calculates the quantity of gas, dX (μg), that moves through a cross-sectional area, A (m^2), along a diffusion channel in a specific length of time dt (s) (Dhammapala, 1996, Martins, 2009, Swartz, 2016).

$$\Phi = \frac{\left(\frac{dX}{dt}\right)}{A} \tag{2.26}$$

Integrating, simplifying, and rearranging **Equation 2.25** and **Equation 2.26** result in **Equation 2.27** (Dhammapala, 1996, Martins, 2009, Swartz, 2016). The C_{avg} derived from **Equation 2.27** is stated in mixing ratios, which represent the volume (mm^3) of pollutant gas per volume (m^3) of moist air under sampling conditions. This expression is used to remove the influence of pressure on the measurement (Dhammapala, 1996, Martins, 2009, Swartz, 2016).

$$C_{avg} = \left(\frac{X}{D \cdot t}\right)\left(\frac{L}{A}\right) \quad (2.27)$$

The term $\frac{L}{A}$ may be determined using **Equation 2.28**, which involves adding the thickness (L_X) and area (A_x) of the plastic ring (R), the PTFE filter pores (F), the steel mesh (N), and the static layer (S) (Dhammapala, 1996, Martins, 2009, Swartz, 2016).

$$\frac{L}{A} = \left(\frac{L_R}{A_R}\right) + \left(\frac{L_F}{A_F}\right) + \left(\frac{L_N}{A_N}\right) + \left(\frac{L_S}{A_S}\right) \quad (2.28)$$

It is crucial to emphasise that the calculations consider the inner diameter (21 mm) of the ring, as this is the diameter of the portion where diffusion might occur. On average, the static layer's thickness for outdoor samples is 1.5 mm (Ferm, 1991). The $\frac{L}{A}$ ratio for this arrangement is 35 m^{-1} according to Dhammapala (1996). By applying the ideal gas law to **Equation 2.27**, **Equation 2.29** is obtained (Dhammapala, 1996).

$$C_{avg} = \left(\frac{1000 \cdot X \cdot R \cdot T}{\cdot D \cdot t}\right)\left(\frac{L}{A}\right) \quad (2.29)$$

This equation is utilised to convert the determined concentration of leached pollutants (ppb) into an average concentration during a monthly time period. In **Equation 2.29**, X (µg) represents the amount of the gaseous species trapped on the filter. It is calculated by multiplying the leached concentration (ppb) by the leached volume (dm^{-3}). R represents the gas constant (8.31 $J.K^{-1}$ mol^{-1}). T (K) represents the average temperature during the sampling period. M_r represents the relative molar mass of the gaseous species of interest. D_x represents the diffusion constant of the gaseous species of interest. t (h) represents the sampling period and $\frac{L}{A}$ being calculated by **Equation 2.28** (Martins, 2009, Swartz, 2016). The diffusion constant values utilised in this investigation are presented in **Table 2.3** as was used in previous studies (Dhammapala, 1996, Martins, 2009, Swartz, 2016).

Table 2.3 Diffusion constants for trace gas species.

Trace gas species	D_x ($m^2 \cdot s^{-1}$)
SO_2	1.30×10^{10}
NO_2	1.52×10^{10}
O_3	1.48×10^{10}

The equations shown below (**Equation 2.30 to 2.32**) demonstrate the chemical reactions involved in the process of trapping and quantitatively collecting SO_2, NO_2 and O_3 using passive samplers (Koutrakis et al., 1993, Ferm et al., 1994, Martins, 2009, Swartz, 2016). Therefore, the trace gases of interest are not directly detected, but are analysed as $2SO_4^{2-}$, NO_2^- and NO_3^-respectively.

$$2SO_{2(g)} + 4OH^- + O_2 \rightarrow 2SO_4^{2-} + 2H_2O \quad (2.30)$$

$$2NO_{2(g)} + 3I^- \rightarrow 2NO_2^- + I_3^- \quad (2.31)$$

$$O_{3(g)} + NO_2^- \rightarrow NO_3^- + O_2 \quad (2.32)$$

The SO_3^{2-} is formed by the reaction of SO_2 with OH^- (**Equation 2.30**). The anion SO_3^{2-} undergoes a reaction with O_2 and many other catalytic trace species in the environment, resulting in the formation of the anion SO_4^{2-} (Swartz, 2016).To efficiently capture the volatile NO_2^- ion (**Equation 2.31**), it is necessary to maintain the absorbent at a somewhat elevated pH level. Sodium hydroxide (NaOH) is the optimal choice for this task, as it maintains a pH level of 13 or above. When the pH level is 12 or below, the NO_2^- ions might undergo oxidation to become NO_3^- ions. The injection of extra I^- can prevent atmospheric oxidants from interacting with the reactive NO_2^-. This is because the atmospheric oxidants combine with I^- to generate I_2, thereby removing them from the atmosphere (Swartz, 2016).

Equation 2.32 demonstrates the chemical process that effectively captures O_3 for the purpose of monitoring its atmospheric concentrations. Controlling the pH of the absorbing surface is crucial since the reaction constant for this reaction reaches its highest value when the pH is 12. This is accomplished via the inclusion of potassium carbonate (K_2CO_3). The hygroscopicity of the sorbent crystals (NO_2^-) is another significant element in this process. Their ability to undergo oxidation with O_3 is increased with an increase in hygroscopicity, resulting in a rise in the efficiency of their collection. The hygroscopicity is enhanced by including glycerol ($C_3H_8O_3$) and employing various nitrite and carbonate salts to generate sorbent crystals (Swartz, 2016). Koutrakis et al. (1993) propose that the mechanism by which O_3 is captured involves a homogeneous phase reaction occurring within tiny H_2O droplets on the filter's surface. While it is possible for NO_2^- to undergo oxidation by H_2O_2 the pH of the solution is too elevated, preventing this reaction from taking place. The interaction between HNO_3 and K_2CO_3 also produces NO_3^-, although its contribution to the overall accumulation of NO_3^- is less than 5% due to the relatively low concentration of HNO_3 compared to O_3 (Swartz, 2016).

In certain cases, however, it is necessary to establish a scaling or correction factor for passive samplers to enhance their accuracy and precision (Vardoulakis et al., 2009). Passive samplers may inaccurately estimate atmospheric concentrations of gaseous species, either by underestimating or overestimating, because they do not immediately monitor the concentrations of these species in real time like an active *in situ* sampler does. Gaseous species undergo a chemical reaction with a sorbent in the passive sampler, which captures the specific gaseous species. The captured species are then examined offline. Thus, as stated earlier, it is necessary to consistently assess the effectiveness of these passive samplers in comparison to active *in situ* measurements.

2.10 Active sampling techniques

The Thermo Environmental Instruments (TECO) Model 43S analyser actively analyses the amounts of SO_2 in the. This instrument employs UV fluorescence to detect SO_2 (Rickman, 1990). The principle of this instrument works based on how SO_2 molecules absorb UV light to become excited at one wavelength, when decaying to a lower energy state the molecule emits UV light at a different wavelength as can be seen from **Equation 2.33** where * represents the SO_2 molecule in its excited state (Rickman, 1990, Thermo Fisher Scientific, 2007a).

$$SO_2 + hv_1 \rightarrow SO_2^* \rightarrow SO_2 + hv_2 \quad (2.33)$$

The Teledyne API's Model T200U analyser is utilised for the measurement of NO_x, NO and NO_2 within the atmosphere. This analyser utilises modern microprocessor technology and chemiluminescence detection for monitoring ambient or diluted concentrations of NO_x, NO and NO_2 in CEM applications (Teledyne API, 2019). The chemiluminescence resulting from the interaction between NO and O_3 is utilised by the analyser to quantify the content of NO in the environment. The concentration of NO is subtracted from the NO_x to ultimately get the NO_2 concentration. This reaction occurs in two distinct phases, as illustrated by **Equation 2.34**, where * represents the NO_2 molecule in its excited state, and **Equation 2.35** (Teledyne API, 2019).

$$\mathrm{NO} + \mathrm{O_3} \rightarrow \mathrm{NO_2^*} + \mathrm{O_2} \quad (2.34)$$

$$\mathrm{NO_2^*} \rightarrow \mathrm{NO_2} + \mathrm{hv_{1200nm}} \quad (2.35)$$

The Model 49i UV Photometric O_3 analyser from Thermo Scientific actively measures concentrations of O_3 in the atmosphere. This analyser operates on the principle that O_3 molecules absorb UV light with a wavelength of 254 nm. According to the Beer-Lambert Law (represented by **Equation 2.36**), the quantity of O_3 present is exactly proportional to the extent of absorption of UV radiation (Thermo Fisher Scientific, 2007b).

$$\frac{\mathrm{I}}{\mathrm{I_0}} = \mathrm{e^{-KLC}} \quad (2.36)$$

Where K is the molecular absorption coefficient at 0°C and 1 atmosphere, L the length of the cell (38 cm), C the concentration of ozone (ppm), I referring to the UV intensity of the sample gas (UV intensity of the sample with O_3) and I_0 the UV intensity of the reference gas (UV intensity of the sample without O_3).

Chapter 3

3. METHOD AND MATERIALS

In this chapter the experimental method and analytical techniques followed are described. The measurement site, reagents and materials, the passive and active in situ methods, analytical techniques along with quality assurance and data processing are described in detail.

3.1 Site Description

The Welgegund atmospheric measurement site, established in 2010, was the sampling site for this study and has been described in detail in various other studies (Jaars et al., 2014, Vakkari et al., 2015, Booyens et al., 2015, Räsänen et al., 2017, Jaars et al., 2018) The location of the site within the North West Province of South Africa is presented in **Figure 3.1**. The Welgegund atmospheric measurement site is located approximately 30 km north of Potchefstroom at an elevation of 1480 m above sea level with the coordinates being 26°34'10"S, 26°56'21"E (Beukes et al., 2013). The station is situated on a commercial farm with no large point sources within proximity of the site. Although there are no large pollutant sources within proximity of the site, the site is a regional station impacted by the major pollutant source region in the north-eastern interior of South Africa, which includes Mpumalanga Highveld, Vaal Triangle, western Bushveld Igneous Complex and the Johannesburg-Pretoria megacity (Beukes et al., 2013, Tiitta et al., 2014, Ngoasheng et al., 2021). In addition, Welgegund is also impacted by a relatively clean region to the west of the site (Tiitta et al., 2014, Jaars et al., 2016). The region experienced an average temperature of 17 ºC during the sampling period with the average maximum summer temperatures reaching ~30 ºC and the lowest winter temperatures dropping to ~0 ºC. This region is characterised by a distinct wet and dry season with precipitation mainly occurring during the warmer months, typically from mid-October to mid-May. The station is surrounded by grassland savannah utilised for grazing by livestock such as cattle and sheep (Jaars et al., 2016).

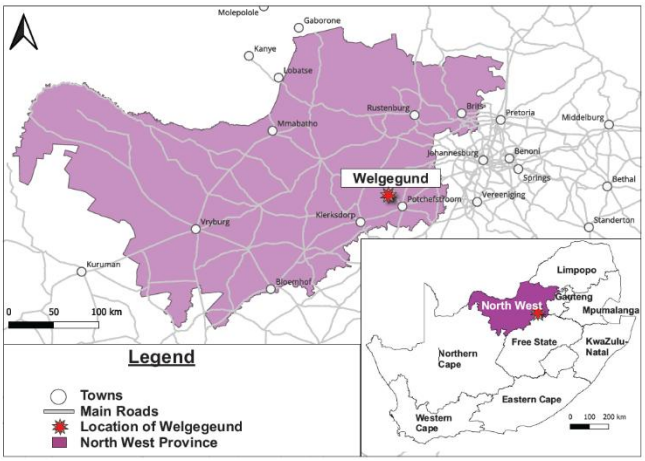

Figure 3.1 Map of the North West province of South Africa with the red star indicating the location of the Welgegund atmospheric monitoring station. A map of South Africa, showing its provinces, is presented at the bottom right.

3.2 Reagents and Materials

Analytical grade reactants and solutions obtained from different suppliers were used in this study, since the highest quality chemicals are crucial when measuring concentrations of atmospheric pollutants. Chemicals were utilised without further purification. Standard stock solutions for calibrations were supplied by Spectrascan®. These standards, which included nitrite (NO_2^-) for nitrogen dioxide (NO_2), sulphate (SO_4^{2-}) for sulphur dioxide (SO_2), and nitrate (NO_3^-) for ozone (O_3), i.e. the atmospheric gaseous species measured in this study, were confirmed to have a purity level of 99.5%. De-ionised water (18.2 $\mu S.cm^{-1}$) was used for the preparation of all aqueous solutions, as well as for rinsing and washing.

The construction of the passive samplers required two types of filter membranes: 25 mm ash-less hardened media filters and 25 mm Teflon® (PTFE) filter membranes with a pore size of 1 micron, both manufactured by Whatman®. The housing of the passive sampler, consisting of the sample cup, support ring, top cap, and stainless-steel mesh was manufactured in-house by the instrument makers at the North-West University (Ferm, 1991, Swartz, 2016). The polypropylene tubes used to construct the top caps were fabricated by Bellco Glass and provided by The Scientific Group (Swartz, 2016).

3.3 Sampling Methods

3.3.1 Passive Sampler Preparation and Assembly

Detailed description of the functioning of passive samplers utilised by the NWU and in this study are presented in Chapter 2 (**Section 2.9**). In this study passive samplers were used to measure atmospheric SO_2, NO_2 and O_3 in order to compare to active *in situ* measurements of these species. An ash-less hardened media filter saturated with 50 µL of the appropriate absorbing solution was placed in the sample cup. All absorbing solutions were prepared in 100 mL volumetric flasks. The absorbing solutions for SO_2 were prepared by dissolving 1.00 g of sodium hydroxide (NaOH) in 5 mL of de-ionised H_2O. For NO_2, the absorbing solution was prepared by dissolving 0.88 g of NaOH and 7.90 g of sodium iodide (NaI) in 5 mL of deionised water after which the flask was filled with methanol (MeOH). The absorbing solution for $O_3$was prepared by dissolving 1.00 g of $NaNO_2$ (which had been dried for 15 minutes at 70 °C) and 1.00 g of K_2CO_3, together with 2 ml of glycerol ($C_3H_8O_3$) in a 7:3 mixture of H_2O and MeOH. Once the ash-less paper filter was saturated with the appropriate absorbent solution, the assembly was completed by fitting the sample cup with a supporting ring, and the top cap with a stainless-steel mesh disc and a PTFE filter as discussed and presented in Chapter 2 (**Section 2.9**, **Figure 2.1**). Passive samplers were prepared and deployed in duplicate, while blank samplers were also prepared for each month of sampling. The prepared passive samplers were placed in airtight containers, stored in airtight bags, and kept in a freezer until the day of exposure.

3.3.2 Passive Sampling

As mentioned above, passive samplers were continuously deployed on a monthly basis at the Welgegund atmospheric measurement station from August 2012 to June 2018. There were analytical uncertainties with passive samples exposed after June 2018, the wrong standards were used for the specific gaseous species in the calibration of the IC. Therefore, this six-year sampling period was utilised in this study for comparison with active *in situ* measurements, which can still be considered as a substantial exposure period to evaluate the performance of the passive samplers. Passive samplers stored in a freezer until the day of deployment, were removed from the bags and placed in the housing unit presented in **Figure 3.2**. These enclosures were located approximately 3 m above the ground on top of one of the containers at Welgegund and comprised of rails specifically designed to accommodate the passive samplers (**Figure 3.2**). As seen in **Figure 3.2** on the right, the samplers were inserted in the rails, with the top assembly oriented downward, exposing the stainless-steel mesh. After the one-month sampling period, passive samplers were removed, placed in bags and airtight containers, and stored in the freezer until analysis.

Figure 3.2 The housing unit used for deployment of passive samplers at Welgegund with the aluminium rails in which the passive samplers were placed shown on the right.

3.3.3 Active *in situ* Measurements

Concentrations of SO_2, NO_2 and O_3 determined with passive samplers were compared with continuous active *in situ* sampling of these species at Welgegund. As mentioned in **Section 2.10** these instruments included the TECO Model 43S analyser for SO_2, the Teledyne API's Model T200U analyser for NO_2 (calculated by using the NO_x and NO concentrations) and the Model 49i UV Photometric ozone analyser for O_3. Measurements of these gaseous species were recorded in intervals of 1 min from which 15-minute average concentrations of SO_2, NO_2 and O_3 were calculated for comparison with passive samplers.

3.4 Analysis of Passive Samplers

Prior to analysis, the hardened ash-less paper filters were removed from the SO_2, NO_2 and O_3 passive samplers (and blanks) and placed in 5 mL, 10 mL and 25 mL deionised water, respectively for 30-minute sonication in an ultrasonic bath. NO_2 passive samplers exposed from August 2017 to March 2018, and April 2018 to June 2018 were subjected to 5 mL and 6 mL deionised water respectively for sonication, after some refinement of the process. The modifications in the leaching of NO_2 passive samplers will be discussed further in the subsequent paragraph.

Analyses of all extracted samples from passive samplers were conducted with the Dionex ICS-3000 IC system. This system comprised two separate flow lines dedicated for the analysis of anion and cation species. In this study, only anionic species were determined, i.e. SO_4^{2-} for SO_2, NO_2^- for NO_2, and NO_3^- for O_3. Some modifications were made to the instrument during the sampling period in an effort to improve and refine the analytical technique. One of these modifications involved switching from a 2 mm system, i.e. a 2 mm AS 18 analytical column, 2 mm AG 18 guard column, 2 mm CRD 200 carbonate removal device, and an ASRS 300 2 mm suppressor to a 4 mm system comprising of a 4 mm AS16 analytical column, 4 mm AG16 guard column, 4 mm CRD 200 carbonate removal device, and an AERS 500 4 mm suppressor (Swartz, 2016). Additionally, the concentration constant and flow rate of the eluent, as well as the applied current, were modified. These changes subsequently led to changes in the leaching volumes for NO_2 passive samples. For every instance where procedures were altered, samples were analysed with both the old and new methods for at least three months, ensuring that the findings obtained from the two approaches could be compared (Swartz, 2016). A potassium hydroxide (KOH) eluent was applied in an isocratic eluent programme during analyses. The IC was calibrated from 1 ppm stock solutions (**Section 3.2**). The analysis of the samples only began after the relative standard deviation of the calibration curve dropped below 5%.

3.5 Quality Assurance

3.5.1 Passive Samplers and Analytical Technique

When quantifying very low concentrations of atmospheric trace elements, maintaining optimal laboratory cleanliness is crucial. Any contamination during preparation or analysis might influence the results. Contamination as small as 20 nmol can lead to a sample inaccuracy of up to 50% (Dhammapala, 1996). Prior to preparing the passive sampler, all components, including the top cap, support rings, sample cup, stainless steel mesh, and reusable PTFE filter discs, were cleaned to prevent contamination. The above-mentioned components were immersed in a 0.2% (v/v) o-H_3PO_4 solution for a maximum of five hours. Afterward, these components were rinsed once and left to soak overnight in a 3% (v/v) EXTRAN MA O2 solution. After this process, all parts of the passive samplers were washed extensively and sonicated in deionised water for about 20 minutes. After being rinsed

three times, the components were then thoroughly dried and stored in airtight containers (Swartz, 2016). All glassware, containers and tools utilised in this study were also cleaned using the same method described above. The ash-less paper filters were cleansed through sonication with methanol (MeOH) for 30 minutes to eliminate any potential impurities and particles. The process was repeated four times after which the filters were allowed to dry and then sealed in airtight bags for storage until deployment. Blanks were also prepared for each batch of passive samplers deployed. Passive samplers and blanks were prepared every three months and stored in a freezer.

The laboratories in which these passive samplers were prepared and analysed were equipped with air filtration systems, which ensured a clean laboratory environment by maintaining positive pressure and eradicating exposure to dust particles. The temperatures of these laboratories were maintained at a constant temperature of 22°C, while the relative humidity was maintained below 40%.

The passive samplers used during this study were evaluated through participation in several inter-comparison studies (Martins *et al.*, 2007). The first comparative study was performed in 1995 by comparison of SO_2, NO_2 and O_3 passive samplers with active *in situ* measurements conducted at the Eskom atmospheric monitoring site, Elandsfontein, located in the Mpumalanga Highveld of South Africa. The study also compared the IVL-based passive samplers developed by the NWU with passive samplers from the Commonwealth Scientific and Industrial Research Organisation (CSIRO) based in Australia (Dhammapala, 1996). From 1998 to 2000, the passive samplers were also compared to active *in situ* measurements conducted at two additional sites, i.e. Palmer and Cape Point (Van der Walt et al., 1998; Swartz et al., 2016). An intercomparison study (initiated by the WMO/GAW Urban Research Meteorology and Environment (GURME) project in collaboration with the International Global Atmospheric Chemistry - Deposition of Biogeochemical Important Trace Species (IGAC-DEBITS) programme) was conducted in 2001 (Carmichael et al., 2003). The most recent intercomparison study was conducted by the University of Singapore in 2008 (He & Bala, 2008), in which the precision and accuracy of SO_2 and NO_2 passive samplers utilised by the NWU were compared to active *in situ* samplers, as well as to passives samplers used by other international institutions. This study indicated that the SO_2 and NO_2 passive samplers utilised by the NWU compared very well to active *in situ* measurements, while having better accuracy compared to similar samplers used by other institutions in most instances. Therefore, as previously mentioned, the main aim of this study was to evaluate how well the passive samplers used by the NWU compare with active *in situ* measurements conducted at Welgegund.

The IC analytical techniques utilised in this study, as well as the pH and conductivity measurements, were also verified by participating in the bi-annual Laboratory Inter Comparison Study of the World Meteorological Organisation (WMO LIS). A sample set comprising three laboratory-prepared samples was analysed and the results published online in ring diagrams. In **Figure 3.3** an example of such a ring diagram with information is presented (QASAC-Americas, 2024). Green hexagons indicate good results (measurements are within the interquartile range (IQR), defined as the 25th to

75th percentile or middle half (50%) of the measurements), green trapezoids indicate satisfactory results (measurements are within the range defined by median ± IQR/1.349), purple trapezoids indicate results not within the satisfactory category, but within a range defined by the median ± 2(IQR/1.349), and red triangles indicate that the results are unsatisfactory (measurements are outside the range defined by the median + 2(IQR/1.349)). Measurements below the detection limit are indicated by an open circle, while an open circle with a slash through indicates that no measurement was reported (QASAC-Americas, 2024). IQR/1.349 is the non-parametric estimate of the standard deviation, sometimes called the pseudo-standard deviation (QASAC-Americas, 2024). Green hexagons with grey fill represent data points that are within the IQR, but do not fulfil the Data Quality Objectives (DQOs) of the WMO (QASAC-Americas, 2024). A result that falls beyond the range of the median ±1 standard deviation, but still satisfies the DQO, is considered an exception to this specification. It is automatically adjusted to a satisfactory result. A green trapezium with grey fill also represents results that do not meet the DQO. A trapezoid or triangle pointing outward indicates that the measurement obtained is too high, while a trapezoid or triangle pointing inward implies too low concentrations (QASAC-Americas, 2024).

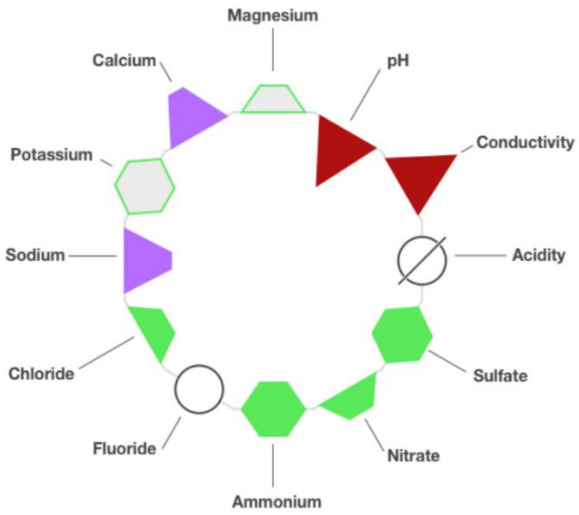

Figure 3.3 Example of a ring diagram visualising WMO LIS results.

In **Figure 3.4**, the ring diagrams of the 68th LIS study in 2023 for the NWU analytical laboratory are presented, which indicate that the IC analytical procedures followed are generally reliable. However, it is evident that there is potential for improvement for certain species, as indicated by the presence of red triangles in all three ring diagrams. It must be mentioned that better WMO LIS results were obtained in previous intercomparison studies e.g. WMO LIS 50 study in 2014 (Conradie et al., 2016) and the WMO LIS 58 study in July 2018 (Swartz et al., 2019). Several factors contributed to observed variabilities in WMO LIS studies conducted over the last couple of years, which were usually due to personnel changes and typical instrumentation errors. According to the WMO inter-comparison results, the recovery of each ion in the standard samples was between 95% and 105%.

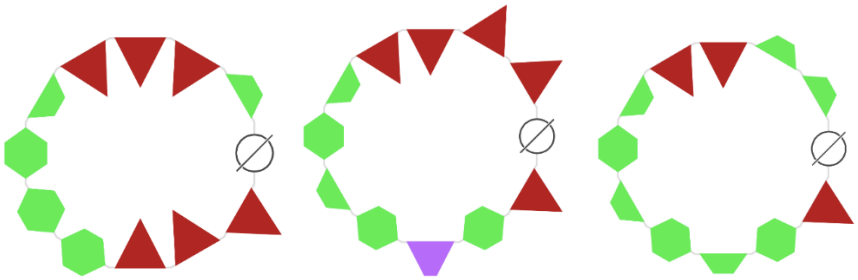

Figure 3.4 Results from the WMO LIS 68 study in 2023 for the NWU laboratory.

3.5.2 Active *in situ* Measurements

The accuracy of the analysers employed in this study can be measured by the instrument drift (Velychko and Gordiyenko, 2023). Drift can be described as an undesirable property of all measuring instruments and can be caused by many factors for example the environment, mechanical vibrations, and temperature changes (Velychko and Gordiyenko, 2023). The span drift of the active analysers used in this study was found to be less than 1% per month for the Model 49i UV Photometric O_3 analyse, <0.5% per day (at constant temperature and voltage) for the Teledyne API's Model T200U NO_x analyser and <0.9% per day for the TECO Model 43S SO_2 analyser (Rickman, 1990, Thermo Fisher Scientific, 2007a, Thermo Fisher Scientific, 2007b, Teledyne API, 2019). To keep the span drift of the instruments low and thus to ensure the reliability and accuracy of the data obtained from the active *in situ* measurements of SO_2, NO_2 and O_3 the analysers were regularly checked and calibrated. Maintenance of instruments at Welgegund was conducted weekly (more often when necessary), while the instruments were calibrated three to four times per year. The one-minute readings of the gaseous species were also adjusted for calibration errors. This adjustment was made by assuming that the reaction of the analyser varied in a linear manner over time. The dataset was evaluated and processed ("cleaned") through utilising a diary that was kept at the site, and visual inspection of the dataset with data associated with errors (experimental, instrumental, human) and uncertainties removed from the dataset. As previously mentioned, the 15-minute mean values were then derived from the 1-minute recorded data. In order to calculate the 15-minute averages, measurements for at least 10 minutes were considered, which means that at least 66.7% of the data had to be available to calculate the 15-minute average.

3.6 Data Processing, Statistical Analysis and Calculations

Data processing and -analysis, as well as statistical assessments were conducted using purpose-specific scripts in programming software MATLAB® R2022b and R statistical language version 4.2.2 (R Core Team, 2022). The MATLAB® scripts used in this study were custom written in all cases in order to conduct the specific tasks required.

The specific R packages used in this study included ggplot2 (version 3.5.0) (Wickham, 2016), tidyverse (version 2.0.0;) (Wickham, 2019), ggstatsplot (version 0.12.2) (Patil, 2021), ggpubr (version

0.6.0) (Kassambara, 2023a), rstatix (version 0.7.2) (Kassambara, 2023b), and ggpmisc (version 0.6.0) (Aphalo, 2024) along with eirasagree package (Silveira et al., 2024). As mentioned in **Chapter 2**, concentrations of ionic species determined with the IC were converted into monthly averages concentrations of SO_2, NO_2, and O_3 (**Equation 2.29**). The average monthly atmospheric concentrations were determined using auxiliary meteorological data, specifically temperature, measured at the Welgegund atmospheric monitoring station.

Active *in situ* measurements of SO_2, NO_2, and O_3 were plotted against the monthly concentrations determined for these species with passive samplers. Cook's distance (D) equation, which is generally used to evaluate the influence of a data point when conducting least squares regression analysis, was utilised to determine outliers (Chatterjee and Hadi, 2012). Large outliers may distort the outcome and accuracy of a regression when comparing active *in situ* measurements with passive data. Cook's distance equation, which is capable of handling large datasets, quantifies the influence of omitting an observation in the correlation plot, and incorporates both the residual and leverage of an observation (Neter et al., 1996, Chatterjee and Hadi, 2012). An observation with Cook's distance more than three times the mean Cook's distance may be regarded as an outlier (Neter et al., 1996). The Cook's distance for an observation i is computed using the equation:

$$D_i = \frac{\sum_{j=1}^{n}(\hat{y}_j - \hat{y}_{j(i)})^2}{p\ MSE} \tag{3.1}$$

where $\hat{y}_j$ denotes the jth expected response value; $\hat{y}_{j(i)}$ signifies the *j*th predicted response value excluding observation i; MSE indicates the mean squared error that measures the average squared deviation between expected and actual data; and p denotes the quantity of coefficients utilised in the regression model. The dataset was visually examined, and outliers removed. The suspected outlier identified by the Cook's distance equation was assessed in relation to other datapoints in the dataset and concentrations determined for a specific species for the same months in other years during the sampling period. In addition, passive data was also removed from the dataset in the absence of any active *in situ* measurements for a specific month.

Since the data was found to be non-normally distributed, several non-parametric analytical tests, i.e. Spearman's correlation, Kruskal-Wallis, and Bland-Altman analyses were performed in order to determine and evaluate scaling factors utilised when calculating atmospheric concentrations SO_2, NO_2, and O_3 with passive samplers after outliers were removed from the dataset. Furthermore, the statistical significance of scaling factors determined in this study in relation to previously used scaling factors for passive samplers was also established.

Scaling factors for the passive samplers were derived from Spearman's correlations between active *in situ* data and passive measurements. In contrast to Pearson's correlation coefficient, the Spearman's correlation does not necessitate the assumption of a linear connection between the variables, nor does it require the variables to be measured on interval scales; it is applicable to

variables assessed at the ordinal level (Hauke and Kossowski, 2011). Since the accuracy of passive samplers were assessed in relation to active *in situ* measurements, SO_2, NO_2, and O_3 concentrations determined with passive samplers were plotted against active *in situ* measurements of these species similarly to previous comparison studies conducted by Dhammapala (1996), Martins (2009), and Adon (2010). The r_s-value (rho) and the p-value derived from the Spearman test also provided valuable insight into the correlation between the active data and the uncorrected passive data.

The Kruskal-Wallis test was employed to compare SO_2, NO_2, and O_3 concentrations determined with active *in situ* measurements to levels determined for these species with passive samplers derived from the previously used and newly determined scaling factors. This *post hoc* analysis utilised a pairwise Dunn's test after establishing statistically significant differences, with p-values corrected through the Benjamini-Hochberg correction for multiple comparisons. Concurrently, epsilon squared (ε^2) was employed to evaluate the effect magnitude.

Spearman's correlation and the Kruskal-Wallis test are frequently employed to examine the correlation between two or more variables. These strategies facilitate the identification of patterns, trends, and/or connections between the variables. However, since these analyses do not provide explicit details on the degree of agreement between the two sampling techniques, Bland-Altman analysis was also performed. This analysis entails plotting the discrepancies between the data acquired from both sampling techniques on the y-axis against the mean of the measurements on the x-axis. This plot might also offer insights into the variability or boundaries of agreement amongst the methodologies. In addition, essential insights into the comparability and interchangeability of sampling techniques are obtained, which enables assessment of the accuracy, precision, and reliability of different methods in relation to each other.

Chapter 4

4. RESULTS AND DISCUSSION

This chapter presents the passive and active in situ concentrations for SO_2, NO_2 and O_3 collected at Welgegund which were used to determine a new scaling factor. A series of statistical tests were performed comparing the old and new scaling factors in order to evaluate them. This chapter also explores the seasonal and inter-annual trends between the passive and active in situ measurements.

4.1 Data Availability

As mentioned in **Section 3.6**, passive data were plotted against active *in situ* measurements and the Cook's distance calculated, which, together with visual inspection, were applied in order to determine outliers that were removed from the dataset. In **Figure 4.1**, Cook's distance calculated for monthly concentrations of SO_2, NO_2 and O_3 determined with passive and active samplers during the sampling period are presented. Also indicated in **Figure 4.1** are all observations exceeding the heuristic threshold considered to be outliers, as these observations are more than three times the mean Cook's distance (Neter et al., 1996). As mentioned in **Section 3.6**, outliers were removed through visual inspection, as well as by considering the datapoint with regard to other datapoints in the dataset, along with concentrations determined for a specific species for the same months in other years. Observations that were in proximity of the heuristic threshold, but not exceeding it, were also inspected and removed where necessary, to prevent deviation from the subsequent linear regression computations. Passive data were also removed from the dataset in the absence of any active *in situ* measurements for a specific month. It is evident from **Figure 4.1** that for SO_2, seven observations were above the heuristic threshold, with three Cook's distances very close to the heuristic threshold, which were considered outliers and removed from the dataset. Six outliers were removed for NO_2, with five observations well above the heuristic threshold and one datapoint within proximity of the heuristic threshold. Seven outliers were identified for O_3 according to Cook's distance calculations, while five more datapoints were removed due to the absence of any active *in situ* measurements. A summary of the data availability used in the subsequent statistical analysis in this study is presented in Table 4.1. It is evident that >80% of the data collected for the three gaseous species could be utilised for further analysis, which can be considered good for the six-year sampling period.

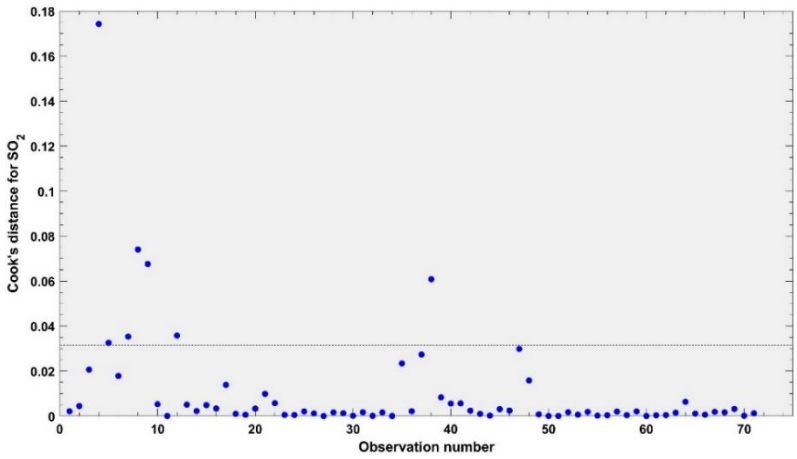

a)

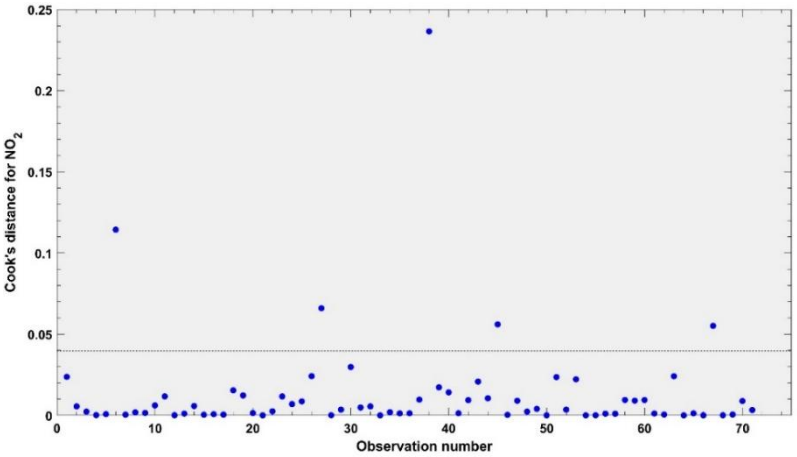

b)

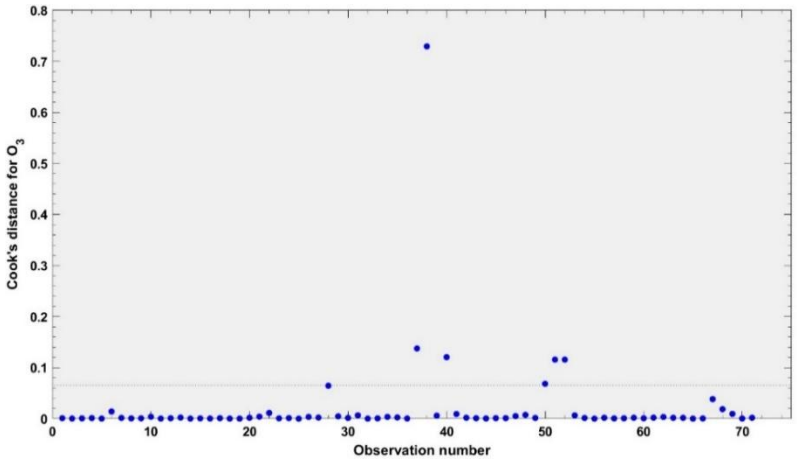

c)

Figure 4.1 Cook's distance calculated for concentrations determined for a) SO_2 b) NO_2 and c) O_3, with passive and active samplers together with the heuristic threshold indicated with a black dotted line.

Table 4.1 Data availability for the sampling period after removing outliers and data for months for which no active measurements were conducted.

Gaseous species	Total number of samples collected	Total number of outliers	Total number of samples retained	Percentage of samples retained
SO_2	71	10	61	85.92%
NO_2	71	6	65	91.55%
O_3	71	12	59	83.10%

4.2 Spearman's Correlations (linear regression)

As previously mentioned, Spearman's correlation was used as a nonparametric test (as the data for all three gaseous species was found to have non-normal distribution) to assess the linear relationship (r_s- and p-value) between the concentrations determined with the unscaled passive samplers and the active *in situ* measurements. The scaling factor could then also be calculated from the slope of linear plots (passing through the origin) of the SO_2, NO_2, and O_3 concentrations, determined with the passive samplers against the active *in situ* measurements, which are presented in **Figure 4.2**. The average ratios between SO_2, NO_2, and O_3 concentrations determined with passive samplers in relation to active *in situ* measurements were 1:1.1, 1:0.6 and 1:0.7, respectively. Therefore, the newly established scaling factors for SO_2, NO_2, and O_3 passive samplers are 0.9, 1.7 and 1.4, respectively, as calculated from the slope of the plots. Previous studies of Dhammapala (1996) and Martins (2009) calculated ratios of approximately ~1:1 for SO_2, ~1:0.6 and ~1:0.7 for NO_2, and 1:08 for O_3 with scaling factors of 1, 1.5 and 1.3 for SO_2, NO_2, and O_3 respectively, when comparing passive data with active measurements. Therefore, it is evident that the correlations between SO_2, NO_2, and O_3 levels determined with passive samplers along with active *in situ* measurements at Welgegund in this study, are in the same order as determined in previous studies. However, as will be shown in subsequent sections, it is suggested that these newly derived scaling factors derived for SO_2, NO_2, and O_3 passive samplers in this study should be used in future research when utilising the passive samplers manufactured by the North-West University (NWU).

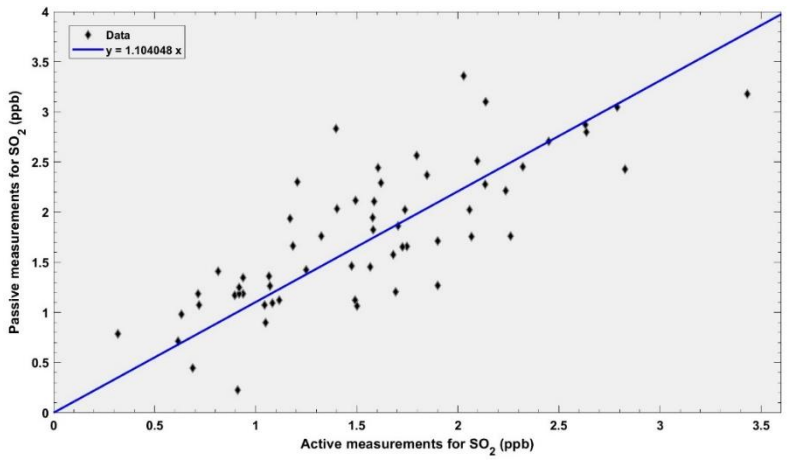

a)

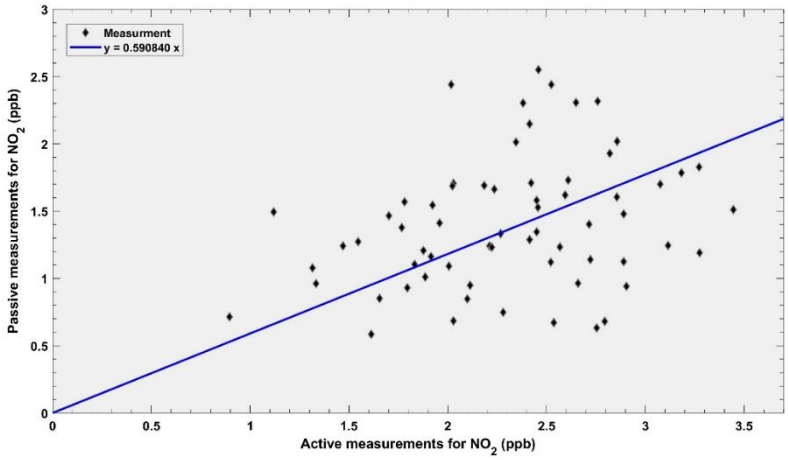

b)

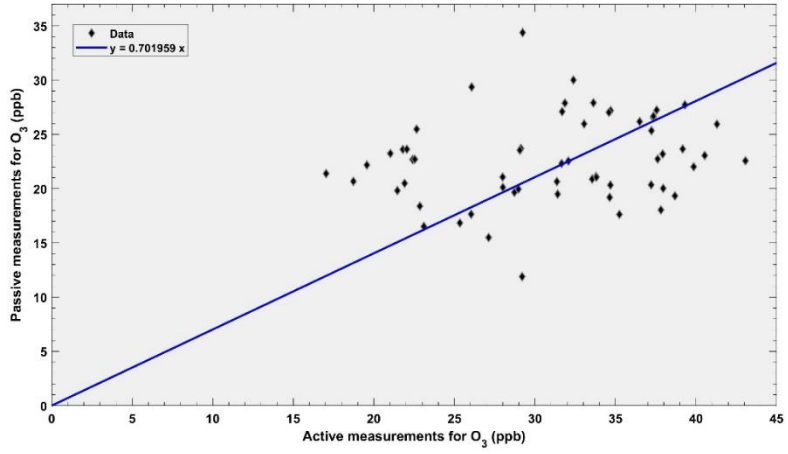

c)

Figure 4.2 Comparison of active in situ measurements with the uncorrected passive measurements for a) SO_2 b) NO_2 and c) O_3 sampled at Welgegund between August 2012 to June 2018.

The minor differences in the scaling factors determined in this study compared to previous studies may be attributed to various factors. Martins (2009) attributed observed differences between passive and active O_3 measurements to the indirect passive sampling of O_3, which measures the overall

oxidation potential of the atmosphere with lower O_3 attributed to wall effects (Adon et al., 2010). Moreover, the discrepancies in NO_2 and SO_2 ratios can be attributed to several factors, with the chemistry of the sorbent being a significant contributor. Multiple decomposition and reverse processes for NO_2^- have been identified, leading to the unreliable and inconsistent estimation of NO_2 utilising a passive sampler (Martins et al., 2007, Martins, 2009).

In **Table 4.2**, the r_s- and p-values determined in the comparison between the uncorrected SO_2, NO_2, and O_3 levels determined with passive samplers and active measurements are presented. The magnitude of the correlation shown by the r_s-values were taken as a r_s-value of 0 showing no relationship, a r_s-value between 0.01-0.49 showing a weak relationship, a r_s-value between 0.50-0.69 showing an average relationship while a r_s-value between 0.70-0.99 shows a strong correlation, a r_s-value of 1 shows a complete correlation between method (Ali Abd Al-Hameed, 2022). The r_s-value of 0.792 calculated for SO_2 thus indicates a strong correlation between passive and active sampling even without the scaling factors (Fowler et al., 2013). Lower r_s-values were determined for NO_2 and O_3, i.e. 0.2837 and 0.2198, which is indicative of a relatively weak correlation between passive and active data. However, the studies of Dhammapala (1996) and Martin (2009) showed similar correlations for these species from which scaling factors were derived. The p-values were assessed with a confidence level of 95% (0.05). The p-value for SO_2, i.e. 0.00 ($p<0.05$), indicates a statistically significant correlation between the active data and the uncorrected passive readings, which also supports the scaling factor of approximately 1. The calculated p-value for NO_2 of 0.022 ($p<0.05$) indicates a statistically significant correlation between active sampling and the uncorrected passive sampler data. Finally, the p-value for O_3 was calculated to be 0.0945 ($p>0.05$), reflecting a lack of adequate evidence to assert a significant connection between the active data and the uncorrected passive values. Therefore, in order to make sure the data gathered from the passive sampling method is comparable and more closely resembles the concentrations collected by means of active *in situ* monitoring, it is imperative to adjust the passive data using the identified scaling factors, especially, for NO_2 and O_3.

Table 4.2 r_s- and p-values determined from Spearman's correlations between uncorrected passive data and active in situ measurements.

Gaseous species	r_s-value	p-value
SO_2	0.792	0.000
NO_2	0.284	0.022
O_3	0.220	0.095

4.3 Kruskal-Wallis Test

In **Figure 4.3, 4.4 and 4.5**, the Kruskal-Wallis tests for respectively SO_2, NO_2, and O_3 are presented. In these tests, SO_2, NO_2, and O_3 concentrations determined with active *in situ* measurements (Active) are compared to levels determined for these species with passive samplers derived from the previously used scaling factor (CorrO) (Dhammapala, 1996, Martins, 2009), and newly determined scaling factors (CorrN) (in this study). The inferential statistics, estimation of impact size along with its level of uncertainty, and pairwise comparisons are indicated. These figures combine violin, box, and jittered plots to visually represent the data. These figures provide a thorough and complete perspective on the distribution of the data. The box component of each plot displays descriptive data, which include the 25th and 75th percentiles that are represented by the top and bottom lines, respectively. The median is shown by the centre line and red dot, and the boxplot whiskers represent 95% data coverage, while the axis is interrupted to highlight outliers. The density of observations is indicated by the violin plot with the wider areas suggesting a higher density of data, while the narrower sections reflect a lower density. In these statistical significance tests, the null hypothesis posits that the distributions are comparable or that there are no significant differences, whereas the alternative hypothesis asserts the presence of statistically significant differences between the examined distributions. We employed a significance level, denoted as alpha, of 0.05 to determine the acceptance or rejection of the null hypothesis. A significance level >0.05 was accepted to show no significant differences, while a value <0.05 was accepted to show significant statistical differences.

The Kruskal-Wallis test conducted on the SO_2 data (**Figure 4.3**) indicates that there is no statistically significant difference (p = 0.18) between the active *in situ* measurements and SO_2 levels determined with passive samplers utilising the two scaling factors ($\chi^2_{\text{Kruskal-Wallis}}(2, \text{N} = 183) = 3.43, p = 0.18;\ \hat{\varepsilon}^2 = 0.02$). This is expected, since CorrO is 1, while CorrN is 0.9. The data suggest that around 2% ($\hat{\varepsilon}^2 = 0.02$) of the variance in concentration may be accounted for by the levels of SO_2 that were obtained both actively and passively. The 95% confidence interval for the effect size indicates a 95% likelihood that the actual value of the effect size falls within the range of 1.77e-03 and 1.00. Although no statistically significant differences were found between the methods, a *post hoc* analysis was implemented to further assess pairwise differences in concentrations determined within the different sampling techniques, which is also presented in **Figure 4.3.** This analysis was done, as the aim of this test within the scope of the study was to evaluate which scaling factor aligned the passive measurements most closely with those obtained using the active *in situ* measurements. The results of the *post hoc* analysis show no significant difference when comparing active data to concentrations determined with passive sampling utilising the scaling factor determined in this study (p = 0.56), or when comparing the active data to concentrations determined with passive sampling utilising the previous scaling factor (p = 0.21). However, the small difference between the actively determined concentration and the passive concentrations corrected with the scaling factor found in this study is

smaller than the difference between the active *in situ* measurements and the passives corrected using the old scaling factor. This demonstrates that calculating SO_2 concentrations with the newly determined scaling factor yields better comparison to active *in situ* measurements despite the small difference between the previously used and the new scaling factor for SO_2 passive samplers. This is also reflected through comparison of the median SO_2 concentrations determined with the different sampling techniques. The median determined for active measurements was 1.57 ppb, compared to the median values of 1.56 ppb and 1.71 ppb calculated with the new and previously used scaling factors, respectively. Comparison of the SO_2 concentrations derived from passive samplers with the two scaling factors also indicate no significant differences (p = 0.33).

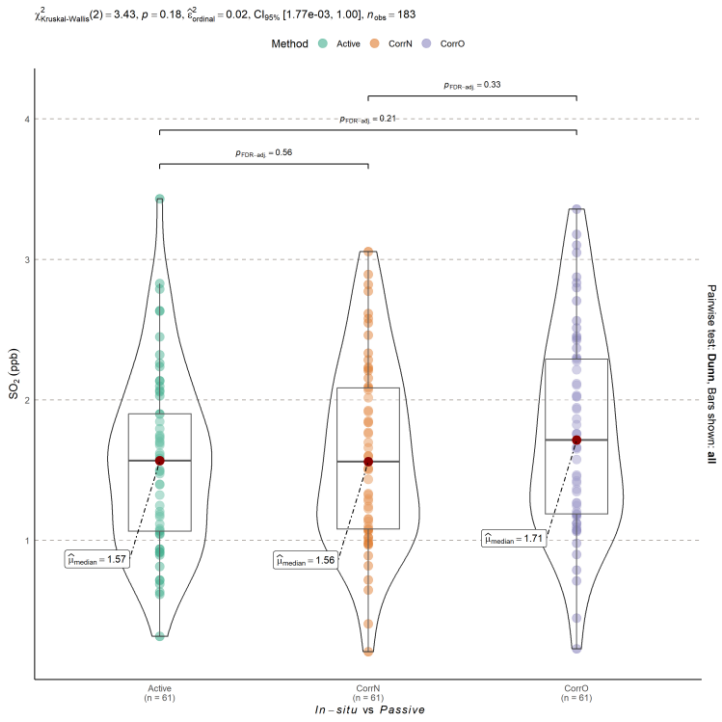

Figure 4.3 A combination of a violin, box and jittered plot of the monthly average SO_2 concentrations determined with the active *in situ* sampler, as well as passive samplers utilising the previously used and new scaling factors determined in this study. Top and bottom line shows the 25th and 75th percentile of concentration, and the middle line and red dot show the median. Whiskers on the boxplots show 95% coverage of the data; the axis is broken along the line to show outliers. The inferential statistics, an estimate of effect size and uncertainty, and pairwise comparisons are also shown.

Figure 4.4 displays the results of the Kruskal-Wallis test conducted for NO_2. The Kruskal-Wallis test reveals no statistically significant differences between the active *in situ* concentrations and NO_2 levels determined with passive samplers using the two scaling factors when taking the alpha value of 0.05 into consideration ($\chi^2_{\text{Kruskal-Wallis}}(2, \text{N} = 195) = 5.36, p = 0.07;\ \hat{\varepsilon}^2 = 0.03$). The $\hat{\varepsilon}^2 = 0.03$ statistic indicates that approximately 3% of the variance in concentration may be accounted for by the levels of NO_2 that were obtained both actively and passively. The 95% confidence interval for

the effect size suggests that there is a 95% probability that the true value of the effect size lies between 4.96e-03 and 1.00. Although no statistically significant differences were found between the methods, a *post hoc* analysis was implemented to further assess pairwise differences in concentrations determined within the different sampling techniques, also presented in **Figure 4.4**. Here no difference is observed when comparing active *in situ* measurements to concentrations determined with passive sampling utilising both the newly determined scaling factor (p = 0.97) or the passive sampler concentrations corrected utilising the previously used scaling factor (p = 0.07). However, the slight difference between the actively determined NO_2 concentration and the passive concentrations corrected with the scaling factor found in this study is much smaller than the difference between the active *in situ* measurements and the passives corrected using the old scaling factor as indicated by the p-value of 0.97 and 0.07 respectively. The higher p-value found between the active concentrations and the passives corrected with the new scaling factor demonstrates that calculating NO_2 concentrations with the newly determined scaling factor yields better comparison to active *in situ* measurements than passive concentrations corrected using the previous correction value. This is also evident when comparing the median values, i.e. 2.38 ppb measured with the active sampler, and 2.27 ppb and 2.02 ppb derived from passive samplers utilising the new and the previously used scaling factor, respectively. However, it appears that the revised scaling factor seems to underestimate the concentration of NO_2 in the atmosphere. Comparison of the NO_2 concentrations derived from passive samplers with the two scaling factors, indicates no difference between the NO_2 levels calculated from passive samplers utilising both scaling factors (p = 0.07).

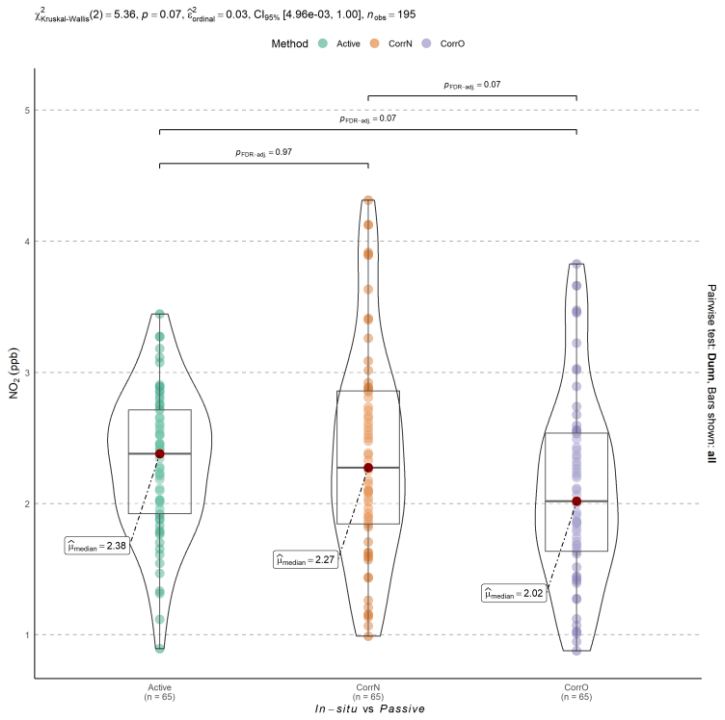

Figure 4.4 A combination of a violin, box and jittered plot of the monthly average NO_2 concentrations determined with the active *in situ* sampler, as well as passive samplers utilising the previously used and new scaling factors determined in this study. Top and bottom line shows the 25th and 75th

percentile of concentration, and the middle line and red dot show the median. Whiskers on the boxplots show 95% coverage of the data; the axis is broken along the line to show outliers. The inferential statistics, an estimate of effect size and uncertainty, and pairwise comparisons are also shown.

The Kruskal-Wallis tests performed for O_3 measurements are presented in Figure 4.5, which indicate statistically significant differences (p = 0.04) between the active in situ measurements and O_3 levels derived from passive samplers with the previously used and the newly determined scaling factors ($\chi^2_{\mathrm{Kruskal-Wallis}}(2, \mathrm{N} = 177) = 6.63, \mathrm{p} = 0.04;\ \hat{\varepsilon}^2 = 0.04$). The data shown by $\hat{\varepsilon}^2 = 0.04$ suggest that around 4% of the variance in concentration may be ascribed to the amounts of O_3 released from both the active and passive method. The 95% confidence interval for the effect size indicates that there is a 95% likelihood that the actual value of the effect size falls within the range of 0.01 to 1.00. Pairwise differences in concentrations determined with the active and passive samplers were also further assessed through post hoc analyses (Figure 4.5). For O_3 no significant difference is observed for O_3 concentrations determined with passive samplers utilising the new scaling factors or for passive concentrations utilising the previous scaling factor when compared to active in situ measurements with p = 0.52 and p = 0.10 respectively. The higher p-value found between the active concentrations and the passives corrected with the new scaling factor demonstrates that calculating O_3 concentrations with the newly determined scaling factor yields better comparison to active in situ measurements than passive concentrations corrected using the previous correction value. Comparison of the O_3 levels derived from passive samplers with the two scaling factors indicates a statistically significant difference (p = 0.33). The median O_3 concentration measured with the active sampler, i.e. 31.87 ppb, whereas the median O_3 levels determined with the new and previously used scaling factors were 32.01 ppb and 29.31 ppb, which also reflects a slight improvement when comparing active in situ measurements with concentrations derived from passive samplers. However, it appears that the new scaling factor marginally overestimates atmospheric O_3 concentrations.

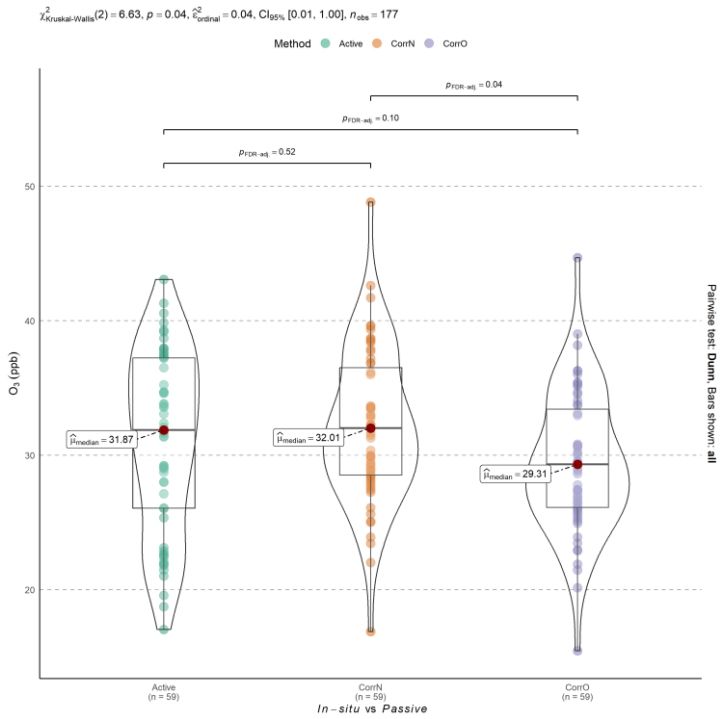

Figure 4.5 A combination of a violin, box and jittered plot of the monthly average O_3 concentrations determined with the active *in situ* sampler, as well as passive samplers utilising the previously used and new scaling factors determined in this study. Top and bottom line shows the 25th and 75th percentile of concentration, and the middle line and red dot show the median. Whiskers on the boxplots show 95% coverage of the data; the axis is broken along the line to show outliers. The inferential statistics, an estimate of effect size and uncertainty, and pairwise comparisons are also shown.

4.4 Bland-Altman Analysis

The SO_2, NO_2, and O_3 concentrations measured with the active *in situ* instruments, and the concentrations of these gaseous species determined with passive samplers utilising the previously used and newly determined scaling factors, were also subjected to Bland-Altman analysis. This statistical method is capable of detecting systematic differences between different sampling techniques, while evaluating the accuracy, precision, and reliability of measurements.

SO_2

In **Figure 4.6** and **Figure 4.7** Bland-Altman analysis evaluating SO_2 concentrations determined with the active sampler in relation to SO_2 levels derived from passive samplers with previously used and new scaling factor, respectively, are presented. From the accuracy plots in **Figure 4.6 a)** and **Figure 4.7 a)**, the (0,0) point representing perfect agreement falls outside the 95% confidence intervals of [0.0947, 0.3423] for active *in situ* measurments in relation to SO_2 levels determined with the previously used scaling factors, while the 95% confidence interval of [-0.0535, 0.1719] determined with the new scaling factor resides within the 95% confidence interval. This suggests a statistically

significant positive bias when using the previously used scaling factor, indicating that the concentrations derived from passive samplers appear to overestimate SO_2 levels in comparison to the active method. However, there is no significant bias when using the new scaling factor. It is also important to note regarding the accuracy of SO_2 levels, that no consistent overestimation or underestimation is seen when comparing these passive measurements to the active *in situ* measurements.

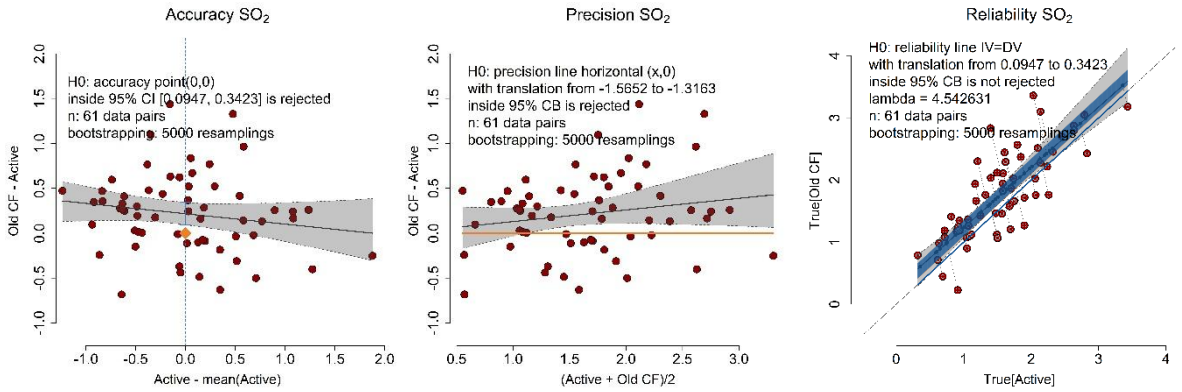

a) b) c)

Figure 4.6 Similarity of a) accuracy, b) precision, and c) reliability for active *in situ* SO_2 measurements in relation to SO_2 concentrations determined with passive samplers utilising the previously used scaling factor obtained using 5×10^3 bootstrap iterations.

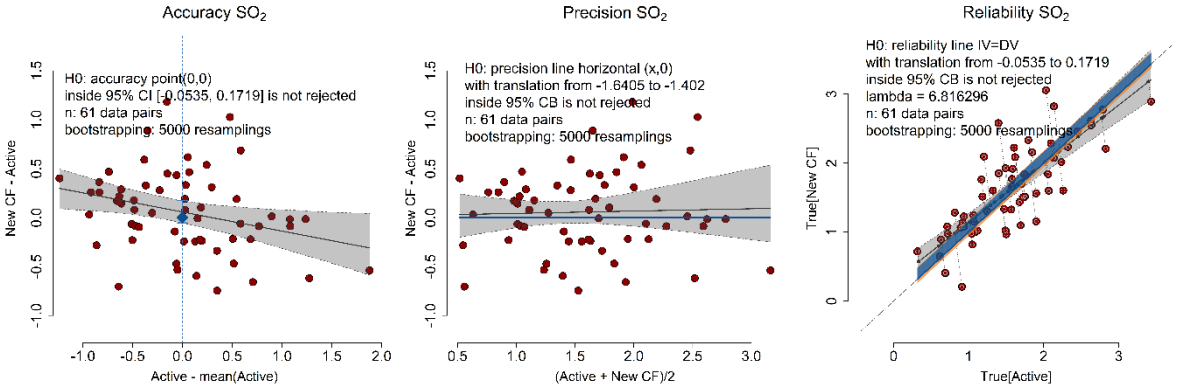

a) b) c)

Figure 4.7 Similarity of a) accuracy, b) precision, and c) reliability for active *in situ* SO_2 measurements in relation to SO_2 concentrations determined with passive samplers utilising the new scaling factor obtained using 5×10^3 bootstrap iterations.

The precision (**Figure 4.6 b)** and **Figure 4.7 b)**) tests depicted for SO_2 levels derived with the previously used scaling factor indicated that the horizontal precision (x, 0) lines were beyond the 95% confidence ranges, hence rejecting the null hypothesis of precision equivalency. However, the precision of passive SO_2 concentrations determined with the new scaling factor resided inside the

95% confidence ranges, reflecting acceptance of the null hypothesis of precision equivalency. Therefore, the precision of the SO_2 levels determined from passive samplers utilising the previously used scaling factors was not statistically relatable to active *in situ* measurements, while passive SO_2 concentrations calculated with the new scaling factor were statistically equivalent to active measurements of this species.

The reliability of the SO_2 passive measurements adjusted according to the previously used scaling factor (**Figure 4.6 c)** and the passive SO_2 levels derived with the new scaling factor (**Figure 4.7 c)**, is statistically significant. For both instances, the bisector line that represents perfect agreement, resides within the 95% confidence intervals, reflecting a high degree of reliability and statistical significance between the SO_2 concentrations derived from passive samplers utilising the previously used and newly determined scaling factors in relation to active *in situ* measurements.

The reliability tests indicated acceptable agreements when comparing active *in situ* measurements to SO_2 concentrations determined with the two scaling factors. However, the precision and accuracy of the SO_2 concentrations derived from passive samplers using the previously used scaling factors revealed some statistically significant biases and lack of precision equivalence. In contrast, the precision and accuracy of the SO_2 concentrations derived from passive samplers using the new scaling factor indicated no rejections or statistically significant differences, strongly supporting the use of the newly determined scaling factors in future research.

NO_2

The Bland-Altman analysis performed for NO_2 measurements (active sampling, as well as passive samplers with previously used and new scaling factors) are presented in **Figure 4.8** and **Figure 4.9**. The (0,0) point in the accuracy analysis for both passive sampling calculations is within the 95% confidence range, which was determined to be [-0.137, 0.2982] when comparing active *in situ* measurements to NO_2 concentrations determined with passive samplers utlising the previous scaling factor and [-0.137, 0.2982] when relating active measurements to NO_2 concentrations determined with the new scaling factor for passive samplers. This suggests no substantial statistical bias between the measurements. Similarly, the accuracy of SO_2 levels, no consistent overestimation or underestimation is seen when comparing these passive measurements to the active *in situ* measurements.

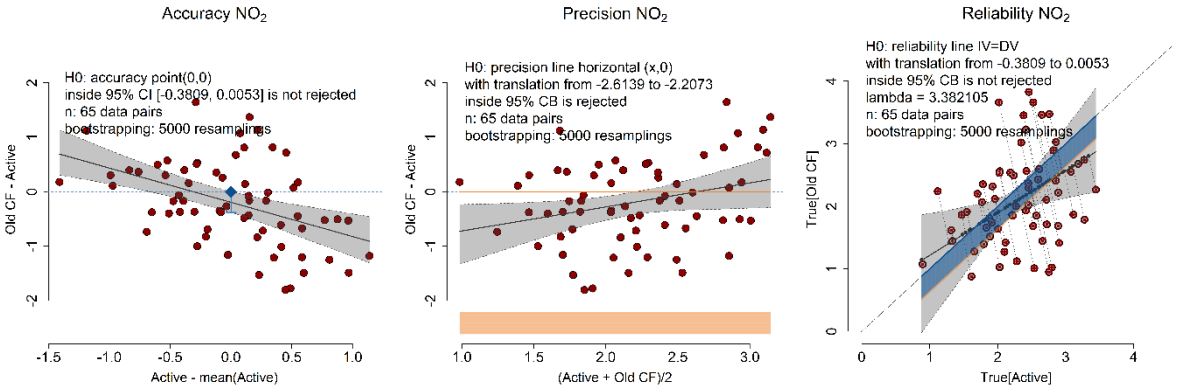

a) b) c)

Figure 4.8 Similarity of a) accuracy, b) precision, and c) reliability for active *in situ* NO_2 measurements in relation to NO_2 concentrations determined with passive samplers utilising the previously used scaling factor obtained using 5×10^3 bootstrap iterations.

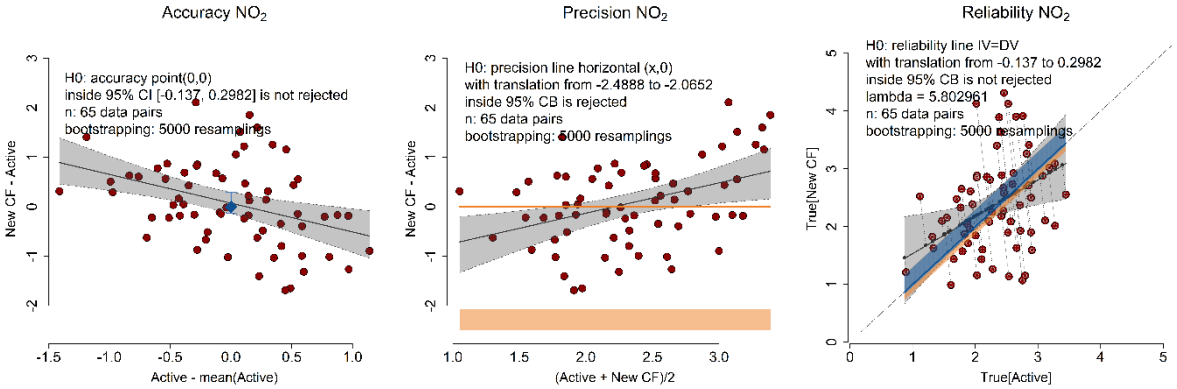

a) b) c)

Figure 4.9 Similarity of a) accuracy, b) precision, and c) reliability for active *in situ* NO_2 measurements in relation to NO_2 concentrations determined with passive samplers utilising the new scaling factor obtained using 5×10^3 bootstrap iterations.

The precision tests for NO_2 levels derived with the previously used scaling factor (**Figure 4.8 b**) and the new scaling factor (**Figure 4.9 b**) indicated that the horizontal precision (x, 0) lines were outside the 95% confidence ranges, which therefore also rejects the null hypothesis of precision equivalency. Therefore, the precision of the NO_2 levels calculated from passive samplers with the previously used and newly determined scaling factors were not statistically equivalent to the NO_2 concentration determined by the active *in situ* measurements.

Signifiicant reliability is evident when relating active NO_2 data to NO_2 concentrations derived from passive samplers utilising both scaling factors, as is evident from (**Figure 4.8 c)** and (**Figure 4.9 c)**. The bisector line resides within the 95% confidence intervals, i.e. perfect agreement, which is indicative of strong reliability and statistical significance between the NO_2 concentrations derived

from passive samplers utlising the previously used and newly determined scaling factors compared to active *in situ* measurements.

The accuracy and reliability tests indicate no rejections or significant statistical discrepancies when relating active NO_2 sampling to NO_2 levels determined with passive samplers for both scaling factors. However, the Bland-Altman analysis did show the comparison of active and passive sampling was not in all instances precise. Overall it can be concluded that NO_2 concentrations derived from passive samplers with the newly determined scaling factor compared well to active *in situ* measurements of these species.

O_3

In **Figure 4.10** and **Figure 4.11** accuracy, precision and reliability tests determined for O_3 levels compared O_3 concentrations derived from passive samplers for the previously used and new scaling factor are presented, respectively. From the accuracy plots in these figures (**Figure 4.10 a)**) the (0,0) point (indicative of perfect concordance) for O_3 concentrations calculated with the previous scaling factors lies outside the 95% confidence interval of [-3.1467, -0.1693]. This suggests a statistically significant negative bias, which indicates that the concentrations obtained with passive samplers adjusted with the previous scaling factor appear to underestimate O_3 concentrations in comparison to the active *in situ* method. O_3 levels determined with the new scaling factor (**Figure 4.11 a)** showed perfect agreement with active *in situ* measurements and resided within the 95% confidence interval of [-0.05709, 2.6814]. Therefore, there is no significant bias when using the newly determined scaling factor. Here it is also imporant to note that no consistent overestimation or underestimation is evident when comparing these passive measurements to the active *in situ* measurements.

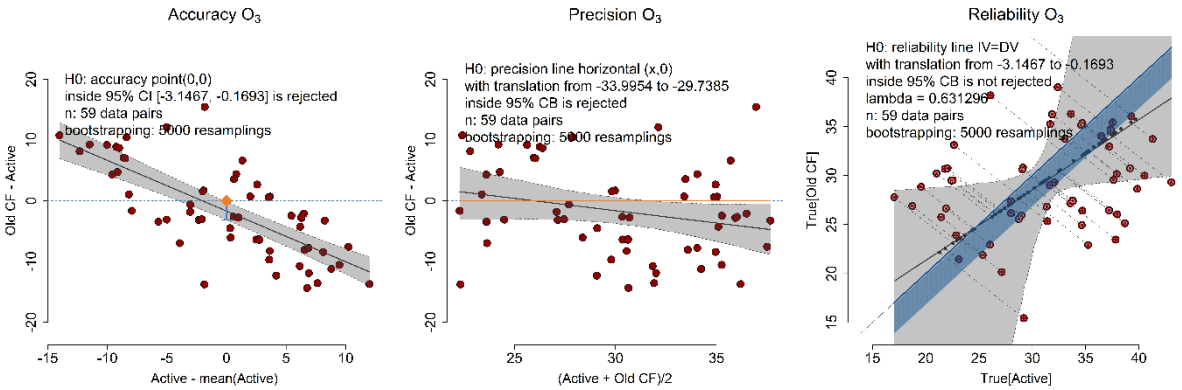

a) b) c)

Figure 4.10 Similarity of a) accuracy, b) precision, and c) reliability for active *in situ* O_3 measurements in relation to O_3 concentrations determined with passive samplers utilising the previously used scaling factor obtained using 5×10^3 bootstrap iterations.

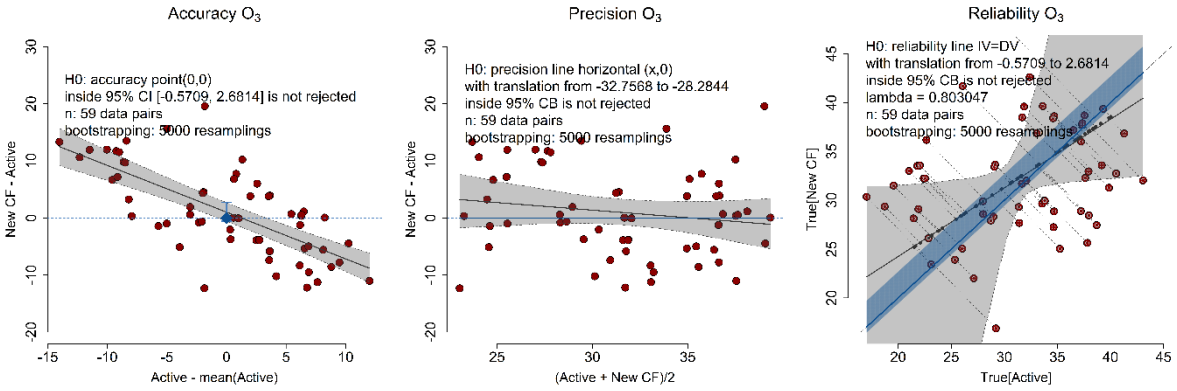

a) b) c)

Figure 4.11 Similarity of a) accuracy, b) precision, and c) reliability for active *in situ* O_3 measurements in relation to O_3 concentrations determined with passive samplers utilising the new scaling factor obtained using 5×10^3 bootstrap iterations.

The precision tests for O_3 concentrations calculated with the previously used scaling factor and (**Figure 4.10 b)** indicated that the horizontal precision (x, 0) lines fell outside the 95% confidence range, which therefore refuted the null hypothesis of precision equivalency. However, the precision of passive O_3 concentrations determined with the new scaling factor and (**Figure 4.11 b**) was inside the 95% confidence range. Therefore, the precision of the O_3 levels determined from passive samplers utilising the previously used scaling factors were not statistically relatable to active *in situ* measurements, while passive O_3 concentrations calculated with the new scaling factor were statistically equivalent to active measurements of this species.

It was also determined that the reliabilities of the O_3 concentrations derived from passive samplers utilising the previously used (**Figure 4.10 c)** and the new scaling factor (**Figure 4.11 c)** were statistically significant. The bisector line that represents perfect agreement resides within the 95% confidence intervals in both instances, indicating strong reliability between the O_3 concentrations derived from passive samplers utilising the previously used and newly determined scaling factors in relation to active *in situ* measurements.

The reliability tests indicated acceptable agreements and no rejections when comparing active *in situ* measurements to O_3 concentrations determined with the two scaling factors. The precision and accuracy of the O_3 concentrations derived from passive samplers using the previously used scaling factors, however, indicated statistically significant discrepancies between the two sampling methods. The precision and accuracy of the O_3 concentrations derived from passive samplers using the new scaling factor indicated no rejections or statistically significant differences for precision and accuracy, which supports the use of the newly determined scaling factors when measuring atmopsheric O_3 with passive samplers.

4.5 Temporal Patterns

4.5.1 Seasonal

In order to further evaluate the performance of passive samplers to determine the concentrations of SO_2, NO_2 and O_3 with passive samplers utilising the new scaling factor established in this study, the monthly concentrations determined for these species with passive samplers were also compared to the seasonal pattern measured with the active *in situ* sampler. The monthly SO_2 concentrations determined with passive samplers utilising the new scaling factor and active *in situ* measurements are presented in **Figure 4.12**. As expected, a similar seasonal pattern is observed for both sampling techniques with good correlations between monthly concentrations. SO_2 concentrations were the highest in winter months, which is typical for the highly industrialised and densely populated north-eastern interior of South Africa. Higher SO_2 concentrations in winter in this part of South Africa is usually attributed to changes in meteorological patterns and source contributions (Lourens et al., 2011, Swartz et al., 2019, Ngoasheng et al., 2021). However, the winter SO_2 peaks are not that prominent compared to measurements within the source regions impacting Welgegund (Stenden et al., 2019), which can be ascribed to Welgegund being a regional background station, as dilution can occur during the travel and aging of air masses after traversing the Vredefort Dome (source regions) prior to reaching Welgegund (Dunn, 2015). Since the main aim of this study was to compare concentrations of inorganic gaseous species measured with passive and active samplers, in-depth assessment of observed seasonal patterns were beyond the scope of this study. The differences between average monthly SO_2 concentrations determined with the two sampling techniques were <15% with the exception of September with a slightly larger difference (20.16%). Medians determined with both sampling techniques had differences <20%, while September showed a 32% difference. Differences were also observed when comparing the monthly statistical distributions of SO_2 levels determined with passive and active sampling, which were expected due to different sampling resolutions of the two methods.

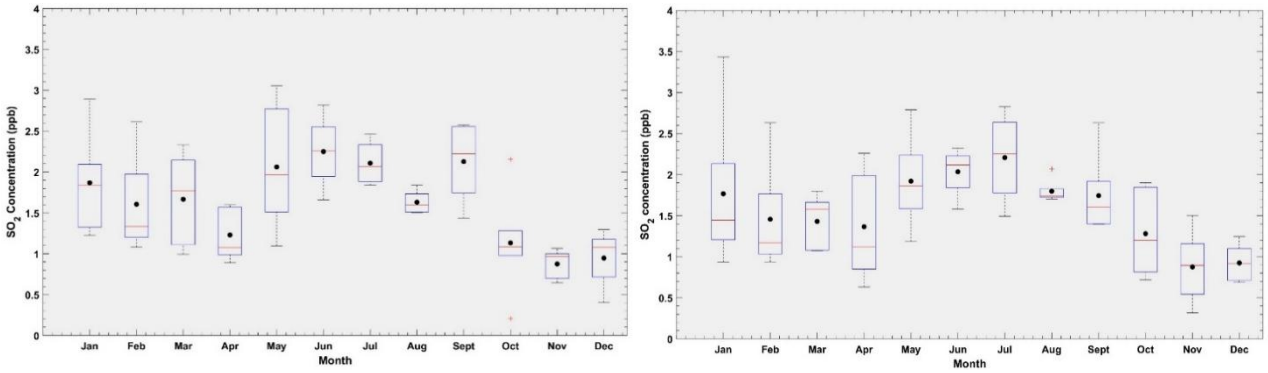

a) b)

Figure 4.12 Monthly SO_2 concentrations measured at Welgegund from August 2012 to June 2018 with (a) passive samplers utilising the new scaling factor, and (b) with active *in situ* samplers. The

red line of each box represents the median, the top and bottom edges of the box the 25th and 75th percentiles, respectively, the whiskers ±2.7σ (99.3% coverage if the data has a normal distribution) and the black dots the averages.

In **Figure 4.13** monthly NO_2 concentrations determined with the two sampling techniques are indicated. In general, similar NO_2 seasonal trends are observed with relatively good correlation between monthly concentrations determined with both sampling techniques. Although higher NO_2 levels were determined during June with the active sampler, the seasonal NO_2 trend at Welgegund does not reflect the influence of pollutant build-up in winter and open biomass burning season in late winter and early spring, which is typically observed in the north-eastern interior of South Africa (Lourens et al., 2011, Stenden et al., 2019). This can be attributed to Welgegund being a regional atmospheric monitoring site, which is not located within a source region. Higher NO_2 concentrations were determined in the warmer months from January to March, which are especially pronounced in the seasonal pattern determined with passive samplers. This is indicative of microbial activity being an important source of NO_2 at Welgegund (Stenden et al., 2019). The differences between average monthly NO_2 concentrations determined with the two sampling techniques were <26%, with the highest percentage difference determined in March. Comparison of the monthly median concentrations determined with passive and active sampling revealed differences ranging from 0.48% in July to 41.40% in October. Similarly, then for SO_2, monthly statistical distributions of NO_2 levels determined with passive and active samplers also exhibited differences.

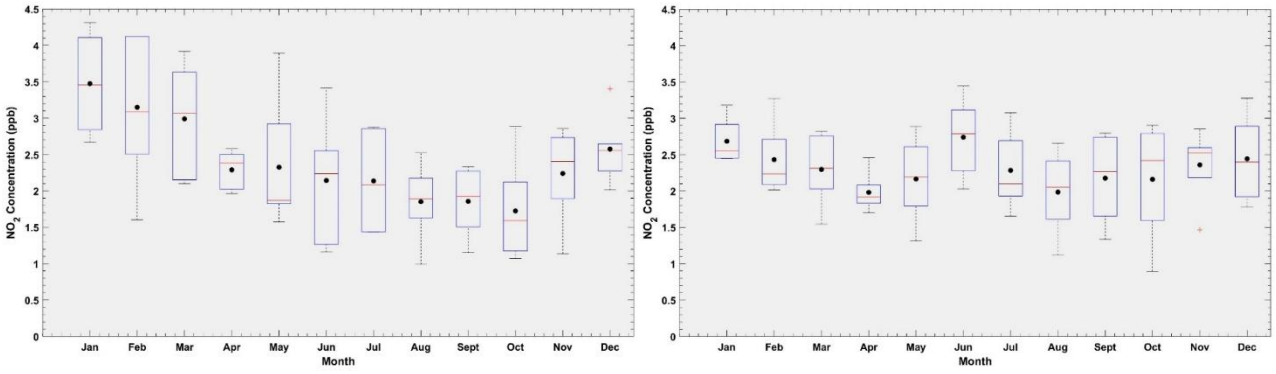

a) b)

Figure 4.13 Monthly NO_2 concentrations measured at Welgegund from August 2012 to June 2018 with (a) passive samplers utilising the new scaling factor, and (b) with active *in situ* samplers. The red line of each box represents the median, the top and bottom edges of the box the 25th and 75th percentiles, respectively, the whiskers ±2.7σ (99.3% coverage if the data has a normal distribution) and the black dots the averages.

Comparison of the monthly O_3 concentration derived from passive samplers with the new corrections and active *in situ* measurements are presented in **Figure 4.14**. Although relatively large differences are observed in the statistical distributions of O_3 levels determined with passive and active

sampling, which is expected due to different sampling resolutions of the two methods, good correlations are observed between average and median O_3 levels determined with the two methods. The differences between average monthly O_3 concentrations determined with the two sampling techniques were <16%, with the exception of the highest percentage difference determined in January, i.e. 28%. Comparison of the median O_3 concentrations with the two sampling methods revealed differences <16%, also with the exception of January that had a median concentration of 27%. Therefore, meaurement of O_3 with passive samplers utilising the new scaling factor can be considered reliable in field measurements. Monthly variability in O_3 concentrations is expected due to the influence of increased household combustion for space heating and cooking in winter, as well as open biomass burning during late winter and early spring in this part of South Africa (Laban et al., 2018, Swartz et al., 2020a). In general, a similar seasonal trend is evident with both sampling techniques, although, as mentioned above, not that evident from the statistical distribution plots in **Figure 4.14**. The highest average and median O_3 concentrations were determined from June to October at Welgegund with both sampling methods, with the exception of higher O_3 levels determined for January with passive samplers. Laban et al., (2018) also reported higher O_3concentrations in January for Welgegund. However, O_3 concentrations at Welgegund remain relatively high throughout the year, which can be attributed to the site being a regional site impacted by aged air masses. As previously mentioned, in-depth assessment of seasonal trends were beyond the scope of this study and were therefore not further explored.

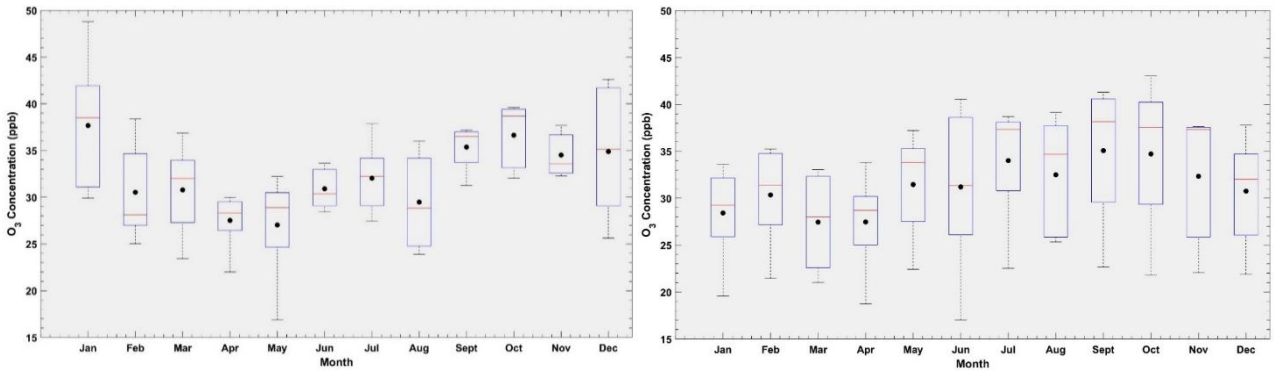

a) b)

Figure 4.14 Monthly O_3 concentrations measured at Welgegund from August 2012 to June 2018 with (a) passive samplers utilising the new scaling factor, and (b) active *in situ* samplers. The red line of each box represents the median, the top and bottom edges of the box the 25th and 75th percentiles, respectively, the whiskers ±2.7σ (99.3% coverage if the data has a normal distribution) and the black dots the averages.

4.5.2 Inter-Annual

The inter-annual fluctuations of SO_2, NO_2 and O_3 concentrations determined with passive- (utilising the new scaling factor) and active sampling were also assessed. Inter-annual variability can also be

ascribed to changes in meteorological conditions and/or variances in source contribution. Swartz et al., (2020), for instance, reported long-term trends of atmospheric SO_2, NO_2 and O_3 measured at three sites in north-eastern interior of South Africa. Relatively large inter-annual variability was reported for SO_2 and NO_2, while O_3 concentrations remained relatively constant through the sampling periods at these three sites. A decrease in levels of atmospheric SO_2 and NO_2 was observed for a certain period, after which concentrations of these species increased for a few years. Inter-annual variability was ascribed to changes in energy demand associated with economic- and population growth. However, as mentioned in the previous section on seasonal trends, detailed evaluation of inter-annual variability of these inorganic gaseous species did not fall within the scope of this study.

The average SO_2 concentration determined with passive samplers during the sampling period was 1.57 ppb, while the mean SO_2 level determined during this period with the active sampler was 1.52 ppb. Similar inter-annual variability was observed for SO_2 concentrations derived from passive samplers compared to SO_2 measurements with the active *in situ* sampler. Both sampling methods showed higher average and median concentrations from 2012 to 2014. The differences between average annual SO_2 concentrations determined with the two sampling techniques were <7% except for 2017 that had a difference of 24%. Medians determined with both sampling techniques had differences <27%, while 2017 revealed a 33% difference. Differences were also observed when comparing the annual statistical distributions of SO_2 levels determined with passive and active sampling, which is expected when comparing these different sampling techniques. The highest average and median SO_2 concentrations determined with passive samplers were 1.79 ppb and 1.88 ppb respectively in 2017, while active *in situ* measurements revealed the highest mean and median SO_2 levels of 1.85 ppb (average and median) in 2013 and 2014. The lowest average and median SO_2 concentrations were determined in 2015 with passive samplers, i.e. 1.39 ppb and 1.15 ppb, respectively. Active *in situ* measurements yielded the lowest mean concentrations of 1.35 ppb in 2012 and 2018, while the lowest median of 1.15 ppb was recorded in 2018.

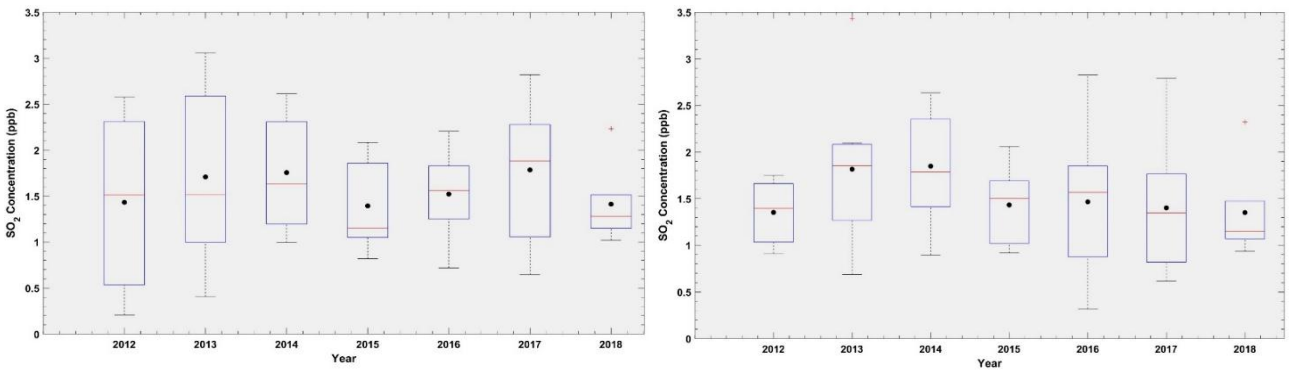

Figure 4.15 Annual SO_2 concentrations measured at Welgegund from August 2012 to June 2018 with (a) passive samplers utilising the new scaling factor, and (b) active *in situ* samplers. The red line of each box represents the median; the top and bottom edges of the box the 25th and 75th

percentiles, respectively; the whiskers ±2.7σ (99.3% coverage if the data has a normal distribution); and the black dots the averages.

The average NO_2 concentrations determined for the entire sampling period at Welgegund with passive samplers and active *in situ* measurements were determined to be 2.39 ppb and 2.29 ppb, respectively. In addition, similar inter-annual varibility patterns are observed for both sampling techniques when comparing annual mean and median NO_2 concentrations determined each year. Furthermore, average and median annual NO_2 levels were relatively constant throughout the sampling period. The differences between average annual NO_2 concentrations determined with the two sampling techniques were <17% except for 2018 with a difference of 29%. Medians determined with both these sampling techniques had differences <16% with the exception of 2012 that showed a 24% difference. As mentioned above for SO_2, differences were also observed when comparing the annual statistical distributions of NO_2 levels determined with passive- and active sampling. The highest average and median NO_2 concentrations recorded with passive samplers were 2.92 ppb and 2.67 ppb, respectively in 2018. Active *in situ* measurements revealed the highest mean NO_2 levels of 2.41 ppb in 2017 with the highest median concentration of 2.57 ppb determined in 2015. The lowest average and median NO_2 concentrations measured with passive samplers were 1.95 ppb and 1.93 ppb, respectively in 2012, while active *in situ* measurements recorded the lowest mean and median concentrations of 2.19 ppb in 2018 and 2.24 ppb in 2013.

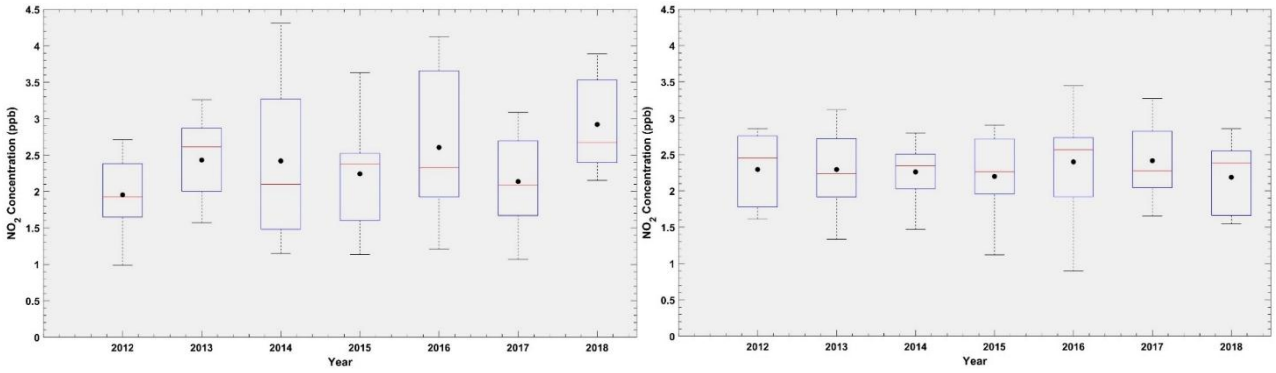

a) b)

Figure 4.16 Annual NO_2 concentrations measured at Welgegund from August 2012 to June 2018 with (a) passive samplers utilising the new scaling factor, and (b) active *in situ* samplers. The red line of each box represents the median; the top and bottom edges of the box the 25th and 75th percentiles, respectively; the whiskers ±2.7σ (99.3% coverage if the data has a normal distribution); and the black dots the averages.

Average O_3 levels determined at Welgegund during the six-year sampling period with passive samplers and active sampling were 32.63 ppb and 34.12 ppb, respectively. As previously mentioned, O_3 data for 2017 and 2018 were not included due to the limited data availability for those two years. Similar inter-annual variability in atmospheric O_3 concentrations was observed for both sampling

techniques. Both sampling methods showed higher O_3 levels measured in 2012 and 2013. The highest average and median O_3 concentrations determined with passive samplers were 34.81 ppb in 2012 and 35.24 ppb in 2013, respectively, while active *in situ* measurements recorded the highest mean and median O_3 levels of 36.85 ppb and 37.62 ppb, respectively, in 2012. The lowest average and median O_3 concentrations were determined in 2014 with passive samplers, i.e. 30.37 ppb and 29.90 ppb, respectively, and active measurements, i.e. 31.16 ppb and 31.36 ppb, respectively. The differences between average annual O_3 concentrations determined with the two sampling techniques were <6%, except for 2015, that had a difference of 14%, while median O_3 concentrations measured with active and passive sampling techniques had differences <13%.

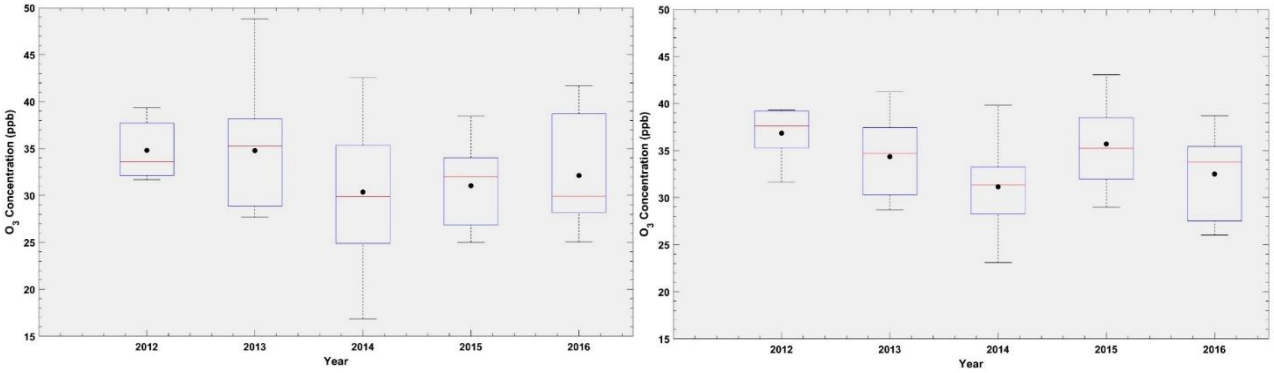

a) b)

Figure 4.17 Annual O_3 concentrations measured at Welgegund from August 2012 to June 2018 with (a) passive samplers utilising the new scaling factor, and (b) active *in situ* samplers. The red line of each box represents the median; the top and bottom edges of the box the 25th and 75th percentiles, respectively; the whiskers ±2.7σ (99.3% coverage if the data has a normal distribution); and the black dots the averages.

Chapter 5

5. CONCLUSION

In this chapter the project is evaluated in terms of successes and shortcomings, while the main conclusions from this study are also presented. Finally, recommendations based on the major findings of this study and future perspectives are discussed.

5.1 Project Evaluation and Main Conclusions

As stated in **Chapter 1**, the general aim of this study was to assess the performance of SO_2, NO_2 and O_3 passive samplers through comparison with active *in situ* measurements of these species conducted at the comprehensively equipped atmospheric measurement station, Welgegund, as well as, if required, to update scaling factors used in the calculations of concentrations of these species determined with passive samplers. In order to achieve this, four specific objectives were identified. Below, this study is evaluated in terms of the success and shortcomings given these objectives, while the major conclusions from this study are presented.

5.1.1 Objective 1

"Deploying SO_2, NO_2 and O_3 passive samplers for a period of at least 5 years at the Welgegund atmospheric monitoring site"

Passive samplers utilised to measure atmospheric SO_2, NO_2 and O_3 concentrations were successfully deployed for ~six years from August 2012 to June 2018 at the comprehensively equipped regional background atmospheric monitoring site, Welgegund. Measurements at Welgegund include active *in situ* measurements of atmospheric SO_2, NO_2 and O_3 levels, along with numerous other parameters (Jaars et al., 2016). Passive samplers were manufactured in-house and deployed monthly at Welgegund. Improvements were made concerning laboratory practices, including preparation (assembling and washing) of the passive samplers. In addition, standard operating procedures were improved, which included the preparation of blanks and updating log sheets to keep track of passive samplers deployed in the field. Furthermore, field protocols were followed meticulously, as no passive sampler exposed during the six-year sampling period, was excluded from the dataset due to sampling errors, with the exception of atmospheric O_3 measured with passive samplers for two months. Therefore, the data coverage percentages were excellent for the six-year sampling period. All passive samplers deployed monthly were successfully analysed with an ion chromatograph (IC) from which atmospheric concentrations of SO_2, NO_2 and O_3 could be calculated with programming software (MATLAB®). The analytical technique was also validated through successful participation in the biannual laboratory inter-comparison study of the World Meteorological Organisation (WMO LIS). The latest result from the WMO LIS (68^{th} LIS study) indicated that the analytical procedures used can be improved to ensure more accurate, precise, and reliable results. As previously mentioned in this study, a limitation associated with passive

samplers relates to the temporal resolution, which allows the measurement of monthly concentrations of atmospheric species. Therefore, instantaneous or momentary peaks in concentrations of these species cannot be identified with passive samplers. However, this study showed that passive samplers can be successfully deployed in data-scarce regions and provide valuable information with regard to general air quality. Although diurnal patterns cannot be measured with passive samplers, seasonal and inter-annual variability in concentrations of SO_2, NO_2 and O_3 can be determined. Although excellent data coverage was achieved for the six-year sampling period given laboratory and field sampling procedures, statistical analyses successfully identified outlier SO_2, NO_2 and O_3 levels, which were excluded from the dataset. However, data availability after statistical assessment SO_2, NO_2 and O_3 were 85.9%, 91.6% and 83.1%, respectively, which can be considered very good. Passive samplers deployed after this six-year sampling period could not be used in this study due to various logistical, instrumental (IC and active *in situ* samplers), and capacity issues experienced from 2018, which resulted in uncertainties and data gaps.

5.1.2 Objective 2

"Processing and analysing active *in situ* measurement datasets determined for these species (SO_2, NO_2 and O_3) at Welgegund during the same sampling period."

The one-minute active *in situ* data recorded for each gaseous species at the Welgegund atmospheric monitoring station were successfully processed utilising a specialised MATLAB® script to yield monthly average concentrations of SO_2, NO_2 and O_3 corresponding to the monthly deployment period for each passive sampler. Additional outliers and unreliable data (e.g. monthly averages with minimal data coverage) were effectively eliminated using the equations and procedures outlined in **Chapter 3** and **Chapter 4**. Excellent data coverage was obtained from active *in situ* measurements during the entire six-year passive sampling period, except for instrumental errors experienced with the O_3 analyser from 2016 to 2018 that resulted in a decrease in the data coverage percentage, as well as exclusion of O_3 data collected for five months during this period in this assessment.

5.1.3 Objective 3

"Determining statistical correlations between passive and active *in situ* measurements in order to verify and/or establish updated scaling factors to calculate the concentrations of these inorganic gaseous species measured with passive samplers."

Spearman's correlation between SO_2, NO_2 and O_3 concentrations determined with passive samplers without any scaling factor, and active *in situ* measurements of these species were successfully performed, from which scaling factors could be derived from the slopes of these correlation plots. Scaling factors established in this study for SO_2, NO_2 and O_3 passive samplers in relation to active *in situ* measurements were 0.9, 1.7 and 1.4, respectively. Kruskal-Wallis and the Bland-Altman tests

were successfully conducted in order to compare SO_2, NO_2 and O_3 concentrations determined with passive samplers utilising the scaling factors determined in this study with active *in situ* measurements, as well as previously used scaling factors for passive samplers. The Kruskal-Wallis pairwise assessment in conjunction with the *post hoc* analysis indicated that SO_2, NO_2 and O_3 levels derived from passive samplers utilising the newly calculated scaling factor, compared well to concentrations of these species measured with the active *in situ* sampling method. The Bland-Altman analysis detects systematic differences between different sampling techniques while evaluating the accuracy, precision, and reliability of measurements. In general, the Bland-Altman test revealed acceptable relations between concentrations determined for these inorganic gaseous species with passive samplers utilising the scaling factors determined in this study and active *in situ* measurements in terms of precision, accuracy and reliability. Weak precision was however determined for NO_2 concentrations derived from passive samplers with the new scaling factor. However, in general, SO_2, NO_2 and O_3 levels determined with passive samplers with the scaling factors determined in this study, performed well in terms of precision, accuracy and reliability compared to concentrations of these species determined with active *in situ* sampling techniques.

5.1.4 Objective 4

"Contextualise and compare correlations determined in this study with previous comparison studies conducted in South Africa and other parts of the world."

Previous scaling factors determined for passive samplers used in this study to measure atmospheric SO_2, NO_2 and O_3 concentrations were 1.0, 1.5 and 1.3, respectively (Dhammapala, 1996, Martins, 2009). Therefore, the correlations between SO_2, NO_2 and O_3 levels determined in this study with passive samplers and active *in situ* measurements at Welgegund are in the same order as previously determined scaling factors with marginal differences. However, as mentioned above, statistical evaluations (Kruskal-Wallis and Bland-Altman tests) revealed that the new scaling factors determined for SO_2, NO_2 and O_3 passive samplers in this study improved the comparison between concentrations of these species determined with passive- and active samplers. The Kruskal-Wallis test for SO_2, NO_2 and O_3, as well as *post hoc* analysis showed that the concentrations of these species corrected with the newly determined scaling factor yielded a closer correlation to the actively determined concentrations than the concentrations derived from passive samplers with the previously used scaling factor. The Bland-Altman analysis also indicated improvements in terms of accuracy and precision when utilising the new scaling factors compared to the previously used scaling factors.

5.2 Recommendations and Future Perspectives

Given the project evaluation presented above, it is evident that new scaling factors derived SO_2, NO_2 and O_3 passive samplers used in this study improved the performance of these passive samplers,

which are therefore recommended to be used in future studies utilising these passive samplers. This study also shows that it is important to keep on deploying passive samplers at Welgegund, allowing for continuous evaluation of the performance of these passive samplers compared to active *in situ* measurement of these species at this location. Furthermore, it is also recommended to participate in inter-laboratory comparison studies in which passive samplers utilised by different laboratories are compared, such as the study conducted by (He and Bala, 2008, Swartz et al., 2020c).

Since the active samplers at Welgegund are checked weekly and calibrated three times per year by an external accredited service provider, a high level of confidence exists in data quality obtained from active *in situ* measurements at Welgegund. However, it is important that the uncertainties associated with these active samplers are determined in future work, which will further improve the accuracy, precision and reliability of passive samplers used in this study.

It is also recommended that passive samplers used in this study are evaluated through comparison with active *in situ* measurements conducted at other locations in South Africa, since changes in the environment and meteorology might also influence the performance of these passive samplers. It is envisaged that active samplers will be deployed at sites in the Expanded Freshwater and Terrestrial Environmental Observation Network (EFTEON), which will allow for comparison of passive samplers with active *in situ* measurements at six sites representative of the different biomes of South Africa.

Future research should also consider assessment of passive samplers utilised to measure atmospheric NH_3, and HNO_3 compared to active measurements of these species. Active measurements of these species are not conducted in South Africa, since instrumentation that performs these measurements is expensive and challenging to operate. However, networks such as EFTEON could provide the necessary infrastructure to conduct these measurements.

References

ABIODUN, B. J., OJUMU, A. M., JENNER, S. & OJUMU, T. V. 2014. The transport of atmospheric NOx and HNO3 over Cape Town. *Atmos. Chem. Phys.,* 14**,** 559-575.

ADLEY, D. P. & UNDERHILL, D. W. 1989. Fundamental factors in the performance of diffusive samplers. *Analytical Chemistry,* 61**,** 843-847.

ADON, M., GALY-LACAUX, C., YOBOUÉ, V., DELON, C., LACAUX, J., CASTERA, P., GARDRAT, E., PIENAAR, J., AL OURABI, H. & LAOUALI, D. 2010. Long term measurements of sulfur dioxide, nitrogen dioxide, ammonia, nitric acid and ozone in Africa using passive samplers. *Atmospheric Chemistry and Physics,* 10**,** 7467-7487.

ALI ABD AL-HAMEED, K. 2022. Spearman's correlation coefficient in statistical analysis. *International Journal of Nonlinear Analysis and Applications,* 13**,** 3249-3255.

AMEDRO, D., BERASATEGUI, M., BUNKAN, A. J., POZZER, A., LELIEVELD, J. & CROWLEY, J. N. 2020. Kinetics of the OH+ NO 2 reaction: effect of water vapour and new parameterization for global modelling. *Atmospheric Chemistry and Physics,* 20**,** 3091-3105.

APHALO, P. S., K. MOUKSASSI, S. 2024. Package 'ggpmisc': miscellaneous extensions to 'ggplot2.

ATKINSON, R. 2000. Atmospheric chemistry of VOCs and NOx. *Atmospheric Environment,* 34**,** 2063-2101.

AYRES, G., CAINEY, J., GILLETT, R. & IVEY, J. 1997. Atmospheric sulphur and cloud condensation nuclei in marine air in the Southern Hemisphere. *Phil. Trans. R. Soc. Lond. B,* 352.

BARKER, J. R. & TINGEY, D. T. 2012. *Air pollution effects on biodiversity*, Springer Science & Business Media.

BEUKES, J. 2019. *Long-term trends of atmospheric SO2, NO2 and O3 concentrations at South African INDAAF sites*, AGU.

BEUKES, J. P., VAKKARI, V., ZYL, P. G. V., VENTER, A. D., JOSIPOVIC, M., JAARS, K., TIITTA, P., KULMALA, M., WORSNOP, D., PIENAAR, J. J., VIRKKULA, A. & LAAKSO, L. 2013. Source region plume characterisation of the interior of South Africa as observed at Welgegund. *Clean Air Journal* [Online], 23.

BLUM, O. & DIDYK, N. 2007. Study of ambient ozone phytotoxicity in Ukraine and ozone protective effect of some antioxidants. *Journal of Hazardous Materials,* 149**,** 598-602.

BOOYENS, W., VAN ZYL, P. G., BEUKES, J. P., RUIZ-JIMENEZ, J., KOPPERI, M., RIEKKOLA, M.-L., JOSIPOVIC, M., VENTER, A. D., JAARS, K. & LAAKSO, L. 2015. Size-resolved characterisation of organic compounds in atmospheric aerosols collected at Welgegund, South Africa. *Journal of Atmospheric Chemistry,* 72**,** 43-64.

BOZKURT, Z., DOĞAN, G., ARSLANBAŞ, D., PEKEY, B., PEKEY, H., DUMANOĞLU, Y., BAYRAM, A. & TUNCEL, G. 2015. Determination of the personal, indoor and outdoor exposure levels of inorganic gaseous pollutants in different microenvironments in an industrial city. *Environ Monit Assess,* 187**,** 590.

BOZKURT, Z., ÜZMEZ, Ö. Ö., DÖĞEROĞLU, T., ARTUN, G. & GAGA, E. O. 2018. Atmospheric concentrations of SO2, NO2, ozone and VOCs in Düzce, Turkey using passive air samplers: sources, spatial and seasonal variations and health risk estimation. *Atmospheric Pollution Research,* 9**,** 1146-1156.

BRASSEUR, G. P., ORLANDO, J. & TYNDALL, G. 1999. Atmospheric chemistry and global change.

BRASSEUR, G. P., SCHULTZ, M., GRANIER, C., SAUNOIS, M., DIEHL, T., BOTZET, M., ROECKNER, E. & WALTERS, S. 2006. Impact of climate change on the future chemical composition of the global troposphere. *Journal of Climate,* 19**,** 3932-3951.

CALVERT, J. G., BOTTENHEIM, J. W. & STRAUSZ, O. P. 1978. Mechanism of the homogeneous oxidation of sulfur dioxide in the troposphere. *Sulfur in the Atmosphere.* Elsevier.

CARMICHAEL, G. R., FERM, M., THONGBOONCHOO, N., WOO, J.-H., CHAN, L. Y., MURANO, K., VIET, P. H., MOSSBERG, C., BALA, R., BOONJAWAT, J., UPATUM, P., MOHAN, M., ADHIKARY, S. P., SHRESTHA, A. B., PIENAAR, J. J., BRUNKE, E. B., CHEN, T., JIE, T., GUOAN, D., PENG, L. C., DHIHARTO, S., HARJANTO, H., JOSE, A. M., KIMANI, W., KIROUANE, A., LACAUX, J.-P., RICHARD, S., BARTUREN, O., CERDA, J. C., ATHAYDE, A., TAVARES, T., COTRINA, J. S. & BILICI, E. 2003. Measurements of sulfur dioxide, ozone and ammonia concentrations in Asia, Africa, and South America using passive samplers. *Atmospheric Environment,* 37**,** 1293-1308.

CHATTERJEE, S. & HADI, A. S. 2012. *Regression analysis by example,* Hoboken, New Jersey, Wiley.
CHEN, D., XU, Y., XU, J., LIAN, M., ZHANG, W., WU, W., WU, M. & ZHAO, J. 2022. The Vertical Distribution of VOCs and Their Impact on the Environment: A Review. *Atmosphere,* 13**,** 1940.
CHEN, T.-M., KUSCHNER, W. G., GOKHALE, J. & SHOFER, S. 2007. Outdoor Air Pollution: Nitrogen Dioxide, Sulfur Dioxide, and Carbon Monoxide Health Effects. *The American Journal of the Medical Sciences,* 333**,** 249-256.
CONNELL, D. W. 2005. *Basic concepts of environmental chemistry*, CRC Press.
DHAMMAPALA, R. S. 1996. *Use of diffusive samplers for the sampling of atmospheric pollutants.*
DIEMINGER, W., HARTMANN, G. K. & LEITINGER, R. 1996. Pollution of the Upper Atmosphere. *In:* DIEMINGER, W., HARTMANN, G. K. & LEITINGER, R. (eds.) *The Upper Atmosphere: Data Analysis and Interpretation.* Berlin, Heidelberg: Springer Berlin Heidelberg.
DUNN, M. 2015. *Characterisation of air masses passing over the Vredefort Dome world heritage site.*
FERM, M. 1991. A sensitive diffusional sampler IVL Report L91-172. *Swedish Environmental Research Institute*.
FERM, M. The theories behind diffusive sampling. Proceedings from the International Conference on Measuring Air Pollutants by Diffusive Sampling, Montpellier, France, 2001. 26-28.
FERM, M., LINDSKOG, A., SVANBERG, P. & BOSTRÖM, C. 1994. New measurement technique for air pollutants. *Kemisk Tidskrift,* 1**,** 30-32.
FERM, M. & RODHE, H. 1997. Measurements of Air Concentrations of SO2, NO2 and NH3 at Rural and Remote Sites in Asia. *Journal of Atmospheric Chemistry,* 27**,** 17-29.
FIELDS, S. 2004. Global Nitrogen: Cycling out of Control. *Environmental Health Perspectives,* 112**,** A556-A563.
FINLAYSON-PITTS, B. J. & PITTS, J. N. 1997. Tropospheric Air Pollution: Ozone, Airborne Toxics, Polycyclic Aromatic Hydrocarbons, and Particles. *Science,* 276**,** 1045-1052.
FINLAYSON-PITTS, B. J. & PITTS JR, J. N. 1993. Atmospheric Chemistry of Tropospheric Ozone Formation: Scientific and Regulatory Implications. *Air & Waste,* 43**,** 1091-1100.
FOWLER, D., PILEGAARD, K., SUTTON, M., AMBUS, P., RAIVONEN, M., DUYZER, J., SIMPSON, D., FAGERLI, H., FUZZI, S. & SCHJOERRING, J. 2009. Atmospheric composition change: ecosystems–atmosphere interactions. *Atmospheric Environment,* 43**,** 5193-5267.
FOWLER, J., COHEN, L. & JARVIS, P. 2013. *Practical statistics for field biology*, John Wiley & Sons.
HAO, J., ZHU, T. & FAN, X. 2018. Indoor Air Pollution and Its Control in China. *In:* PLUSCHKE, P. & SCHLEIBINGER, H. (eds.) *Indoor Air Pollution.* Berlin, Heidelberg: Springer Berlin Heidelberg.
HARRISON, R. M. 1999. *Understanding our environment: an introduction to environmental chemistry and pollution*, Royal Society of chemistry.
HARRISON, R. M. 2013. Chemistry of the troposphere. *Pollution 5th Edition: Causes, Effects and Control,* 5**,** 182.
HAUKE, J. & KOSSOWSKI, T. 2011. Comparison of values of Pearson's and Spearman's correlation coefficients on the same sets of data. *Quaestiones geographicae,* 30**,** 87-93.
HE, J. & BALA, R. 2008. Draft Report on passive sampler inter-comparison under Malé declaration. *Malé Declaration on Control and Prevention of Air Pollution and its Likely Transboundary Effect for South Asia, National University of Singapore, Singapore*.
HEWITT, C. N. 2001. The atmospheric chemistry of sulphur and nitrogen in power station plumes. *Atmospheric Environment,* 35**,** 1155-1170.
HOLMBERG, M., AKUJÄRVI, A., ANTTILA, S., AUTIO, I., HAAKANA, M., JUNTTILA, V., KARVOSENOJA, N., KORTELAINEN, P., MÄKELÄ, A., MINKKINEN, K., MINUNNO, F., RANKINEN, K., OJANEN, P., PAUNU, V.-V., PELTONIEMI, M., RASILO, T., SALLANTAUS, T., SAVOLAHTI, M., TUOMINEN, S., TUOMINEN, S., VANHALA, P. & FORSIUS, M. 2021. Sources and sinks of greenhouse gases in the landscape: Approach for spatially explicit estimates. *Science of The Total Environment,* 781**,** 146668.
JAARS, K., BEUKES, J. P., ZYL, P. G. V., VENTER, A. D., JOSIPOVIC, M., PIENAAR, J. J., VAKKARI, V., AALTONEN, H., LAAKSO, H., KULMALA, M., TIITTA, P., GUENTHER, A., HELLÉN, H., LAAKSO, L. & HAKOLA, H. 2014. Ambient aromatic hydrocarbon measurements at Welgegund, South Africa. 14.

JAARS, K., VAN ZYL, P. G., BEUKES, J. P., HELLÉN, H., VAKKARI, V., JOSIPOVIC, M., VENTER, A. D., RÄSÄNEN, M., KNOETZE, L., CILLIERS, D. P., SIEBERT, S. J., KULMALA, M., RINNE, J., GUENTHER, A., LAAKSO, L. & HAKOLA, H. 2016. Measurements of biogenic volatile organic compounds at a grazed savannah grassland agricultural landscape in South Africa. *Atmos. Chem. Phys.,* 16**,** 15665-15688.

JAARS, K., VESTENIUS, M., VAN ZYL, P. G., BEUKES, J. P., HELLEN, H., VAKKARI, V., VENTER, M., JOSIPOVIC, M. & HAKOLA, H. 2018. Receptor modelling and risk assessment of volatile organic compounds measured at a regional background site in South Africa. *Atmospheric Environment,* 172**,** 133-148.

JEFFRY, L., ONG, M. Y., NOMANBHAY, S., MOFIJUR, M., MUBASHIR, M. & SHOW, P. L. 2021. Greenhouse gases utilization: A review. *Fuel,* 301**,** 121017.

JION, M. M. M. F., JANNAT, J. N., MIA, M. Y., ALI, M. A., ISLAM, M. S., IBRAHIM, S. M., PAL, S. C., ISLAM, A., SARKER, A., MALAFAIA, G., BILAL, M. & ISLAM, A. R. M. T. 2023. A critical review and prospect of NO2 and SO2 pollution over Asia: Hotspots, trends, and sources. *Science of The Total Environment,* 876**,** 162851.

JOSIPOVIC, M., ANNEGARN, H. J., KNEEN, M. A., PIENAAR, J. J. & PIKETH, S. J. 2011. Atmospheric dry and wet deposition of sulphur and nitrogen species and assessment of critical loads of acidic deposition exceedance in South Africa : research article. *South African Journal of Science,* 107**,** 1-10.

KAJINO, M. & AIKAWA, M. 2015. A model validation study of the washout/rainout contribution of sulfate and nitrate in wet deposition compared with precipitation chemistry data in Japan. *Atmospheric Environment,* 117**,** 124-134.

KASSAMBARA, A. 2023a. ggpubr: 'ggplot2' Based Publication Ready Plots.

KASSAMBARA, A. 2023b. rstatix: Pipe-Friendly Framework for Basic Statistical Tests.

KORHONEN, K., GIANNAKAKI, E., MIELONEN, T., PFÜLLER, A., LAAKSO, L., VAKKARI, V., BAARS, H., ENGELMANN, R., BEUKES, J. & VAN ZYL, P. 2014. Atmospheric boundary layer top height in South Africa: measurements with lidar and radiosonde compared to three atmospheric models. *Atmospheric Chemistry and Physics,* 14**,** 4263-4278.

KOUTRAKIS, P., WOLFSON, J. M., BUNYAVIROCH, A., FROEHLICH, S. E., HIRANO, K. & MULIK, J. D. 1993. Measurement of ambient ozone using a nitrite-coated filter. *Analytical Chemistry,* 65**,** 209-214.

LABAN, T. L., VAN ZYL, P. G., BEUKES, J. P., THOMPSON, A. M., NORTH-WEST UNIVERSITY . POTCHEFSTROOM, C., NATIONAL RESEARCH, F. & ATMOSPHERIC CHEMISTRY RESEARCH, G. 2018. *Factors influencing surface ozone variability over continental South Africa and implications for air quality and agriculture*.

LAŠTOVIČKA, J., AKMAEV, R., BEIG, G., BREMER, J. & EMMERT, J. 2006. Global change in the upper atmosphere. *Science,* 314**,** 1253-1254.

LEE, C.-L. & BRIMBLECOMBE, P. 2016. Anthropogenic contributions to global carbonyl sulfide, carbon disulfide and organosulfides fluxes. *Earth-Science Reviews,* 160**,** 1-18.

LIU, Y.-Z., GUO, R.-T., DUAN, C.-P., WU, G.-L., MIAO, Y.-F., GU, J.-W. & PAN, W.-G. 2021. Removal of gaseous pollutants by using 3DOM-based catalysts: A review. *Chemosphere,* 262**,** 127886.

LOURENS, A. S., FOURIE, G. D., BURGER, J. W., PIENAAR, J. J., READ, C. E., JORDAAN, J. H., VAN ZYL, P. G. & BEUKES, J. P. 2011. Spatial and temporal assessment of gaseous pollutants in the Highveld of South Africa. *South African Journal of Science,* 107**,** 1-8.

LOVETT, G. M., TEAR, T. H., EVERS, D. C., FINDLAY, S. E., COSBY, B. J., DUNSCOMB, J. K., DRISCOLL, C. T. & WEATHERS, K. C. 2009. Effects of air pollution on ecosystems and biological diversity in the eastern United States. *Annals of the New York Academy of Sciences,* 1162**,** 99-135.

MANISALIDIS, I., STAVROPOULOU, E., STAVROPOULOS, A. & BEZIRTZOGLOU, E. 2020. Environmental and health impacts of air pollution: a review. *Frontiers in public health,* 8**,** 14.

MARTIN, L. R. & DAMSCHEN, D. E. 1981. Aqueous oxidation of sulfur dioxide by hydrogen peroxide at low pH. *Atmospheric Environment (1967),* 15**,** 1615-1621.

MARTINS, J. J. 2009. *Concentrations and deposition of atmospheric species at regional sites in southern Africa.* North-West University.

MARTINS, J. J., DHAMMAPALA, R. S., LACHMANN, G., GALY-LACAUX, C. & PIENAAR, J. J. 2007. Long-term measurements of sulphur dioxide, nitrogen dioxide, ammonia, nitric acid and

ozone in southern Africa using passive samplers : SAEON review. *South African Journal of Science,* 103**,** 336-342.
MASSARI, S., MIGLIETTA, P. P., DE LEO, F. & RUBERTI, M. 2023. Pollution. *In:* IDOWU, S. O., SCHMIDPETER, R., CAPALDI, N., ZU, L., DEL BALDO, M. & ABREU, R. (eds.) *Encyclopedia of Sustainable Management.* Cham: Springer International Publishing.
MEETHAM, A. R., BOTTOM, D. & CAYTON, S. 2016. *Atmospheric pollution: its history, origins and prevention*, Elsevier.
MENG, Z., XU, X., YAN, P., DING, G., TANG, J., LIN, W., XU, X. & WANG, S. 2009. Characteristics of trace gaseous pollutants at a regional background station in Northern China. *Atmospheric Chemistry and Physics,* 9**,** 927-936.
MONKS, P. & HEY, J. V. 2009. Tropospheric chemistry and air pollution. *Atmospheric science for environmental scientists.* Wiley-Blackwell United Kingdom.
MONKS, P. S., GRANIER, C., FUZZI, S., STOHL, A., WILLIAMS, M. L., AKIMOTO, H., AMANN, M., BAKLANOV, A., BALTENSPERGER, U. & BEY, I. 2009. Atmospheric composition change–global and regional air quality. *Atmospheric environment,* 43**,** 5268-5350.
MONROE, J., WICANDER, R. & HAZLETT, R. 2006. *Physical Geology: Exploring the Earth*, Cengage Learning.
MOZAFFAR, A. & ZHANG, Y.-L. 2020. Atmospheric Volatile Organic Compounds (VOCs) in China: a Review. *Current Pollution Reports* [Online], 6.
NAJJAR, Y. S. 2011. Gaseous pollutants formation and their harmful effects on health and environment. *Innovative energy policies,* 1.
NAMIESNIK, J., GORECKI, T., KOZLOWSKI, E., TORRES, L. & MATHIEU, J. 1984. Passive dosimeters—an approach to atmospheric pollutants analysis. *Science of the total environment,* 38**,** 225-258.
NETER, J., KUTNER, M. H., NACHTSHEIM, C. J. & WASSERMAN, W. 1996. Applied linear statistical models.
NGOASHENG, M., BEUKES, J. P., VAN ZYL, P. G., SWARTZ, J.-S., LOATE, V., KRISJAN, P., MPAMBANI, S., KULMALA, M., VAKKARI, V. & LAAKSO, L. 2021. Assessing SO2, NO2 and O3 in rural areas of the North West Province. *Clean Air Journal,* 31**,** 1-14.
NIU, S., HAN, K. & LU, C. 2011. Release of sulfur dioxide and nitric oxide and characteristic of coal combustion under the effect of calcium based organic compounds. *Chemical Engineering Journal,* 168**,** 255-261.
PATIL, I. 2021. Visualizations with statistical details: The {'ggstatsplot'} approach. *Journal of Open Source Software,* 6**,** 3167.
PELL, E. J. Ozone toxicity—is there more than one mechanism of action? Effects of atmospheric pollutants on forests, wetlands and agricultural ecosystems, 1987. Springer, 229-240.
PETÄJÄ, T., VAKKARI, V., POHJA, T., NIEMINEN, T., LAAKSO, H., AALTO, P., KERONEN, P., SIIVOLA, E., KERMINEN, V.-M. & KULMALA, M. 2013. Transportable aerosol characterization trailer with trace gas chemistry: Design, instruments and verification. *Aerosol and Air Quality Research,* 13**,** 421-435.
PIENAAR, J., BEUKES, J. P., VAN ZYL, P. G., LEHMANN, C. & AHERNE, J. 2015. Passive diffusion sampling devices for monitoring ambient air concentrations. *Comprehensive analytical chemistry.* Elsevier.
PÖSCHL, U. 2005. Atmospheric aerosols: composition, transformation, climate and health effects. *Angewandte Chemie International Edition,* 44**,** 7520-7540.
QASAC-AMERICAS. 2024. *Definitions and DQOs* [Online]. Available: https://qasac-americas.org/definitions [Accessed 17 July 2024].
R CORE TEAM 2022. A language and environment for statistical computing. Vienna, Austria.
RÄSÄNEN, M., AURELA, M., VAKKARI, V., BEUKES, J. P., TUOVINEN, J. P., VAN ZYL, P. G., JOSIPOVIC, M., VENTER, A. D., JAARS, K., SIEBERT, S. J., LAURILA, T., RINNE, J. & LAAKSO, L. 2017. Carbon balance of a grazed savanna grassland ecosystem in South Africa. *Biogeosciences,* 14**,** 1039-1054.
RICKMAN, E. E. 1990. *Laboratory and Field Evaluations of Extrasensitive Sulfur Dioxide and Nitrogen Dioxide Analyzers for Acid Deposition Monitoring*, US Environmental Protection Agency, Atmospheric Research and Exposure ….
RITCHIE 2017. *Atmospheric Chemistry: From The Surface To The Stratosphere*, World Scientific Publishing Europe Ltd.

SCHOLES, M., OLBRICH, K. & VAN RENSBURG, E. The environmental impact of atmospheric pollution in the industrial Highveld and adjacent regions: Crops, indigenous vegetation and commercial forests. Workshop: Air pollution and its impacts on the south African Highveld, 1996.
SEIGNEUR, C. 2019. Gaseous Pollutants. *In:* SEIGNEUR, C. (ed.) *Air Pollution: Concepts, Theory, and Applications.* Cambridge: Cambridge University Press.
SEINFELD, J. 2006. Pandis. SN: Chapter 6. *Atmospheric Chemistry and Physics–From Air Pollution to Climate Change, Second Edition ed., John Wiley & Sons, Inc, New Jersey, USA*.
SEINFELD, J. H. & PANDIS, S. N. 2006. *Atmospheric chemistry and physics: From air pollution to climate change*, John Wiley & Sons.
SILVEIRA, P. S. P., VIEIRA, J. E. & SIQUEIRA, J. D. O. 2024. Is the Bland-Altman plot method useful without inferences for accuracy, precision, and agreement? *Revista de Saúde Pública,* 58**,** 01.
SKOOG, D. A. & WEST, D. M. 1963. Fundamentals of analytical chemistry. *(No Title)*.
SLEZAKOVA, K., PIRES, J. C. M., MARTINS, F. G., PEREIRA, M. C. & ALVIM-FERRAZ, M. C. 2011. Identification of tobacco smoke components in indoor breathable particles by SEM–EDS. *Atmospheric Environment,* 45**,** 863-872.
STEIN, L. Y. & YUNG, Y. L. 2003. PRODUCTION, ISOTOPIC COMPOSITION, AND ATMOSPHERIC FATE OF BIOLOGICALLY PRODUCED NITROUS OXIDE. *Annual Review of Earth and Planetary Sciences,* 31**,** 329-356.
STENDEN, F. H., VAN ZYL, P. G., BEUKES, J. P. & NORTH-WEST UNIVERSITY . POTCHEFSTROOM, C. 2019. *Atmospheric SO^{2-}_2 and NO^{2-}_2 flux measurements at a savannah-grassland-agriculture landscape in South Africa.*
SU, C., RAN, X., HU, J. & SHAO, C. 2013. Photocatalytic Process of Simultaneous Desulfurization and Denitrification of Flue Gas by TiO2–Polyacrylonitrile Nanofibers. *Environmental Science & Technology,* 47**,** 11562-11568.
SWARTZ, J.-S., VAN ZYL, P., BEUKES, J., LABUSCHAGNE, C., BRUNKE, E.-G., PORTAFAIX, T., GALY-LACAUX, C. & PIENAAR, J. 2020a. Twenty-one years of passive sampling monitoring of SO2, NO2 and O3 at the Cape Point GAW station, South Africa. *Atmospheric Environment,* 222**,** 117128.
SWARTZ, J. 2016. *Long-term measurements of concentration and dry deposition of atmospheric inorganic gaseous species at Cape Point, South Africa.*
SWARTZ, J., VAN ZYL, P. G., BEUKES, J. P., NORTH-WEST UNIVERSITY . POTCHEFSTROOM, C., NATIONAL RESEARCH, F. & CENTRE NATIONAL DE LA RECHERCHE, S. 2019. *Long-term trends of ambient gaseous concentrations at South African DEBITS sites and wet deposition at Cape Point.*
SWARTZ, J. S., VAN ZYL, P. G., BEUKES, J. P., LABUSCHAGNE, C., BRUNKE, E. G., PORTAFAIX, T., GALY-LACAUX, C. & PIENAAR, J. J. 2020b. Twenty-one years of passive sampling monitoring of SO2, NO2 and O3 at the Cape Point GAW station, South Africa. *Atmospheric Environment,* 222.
SWARTZ, J. S., ZYL, P. G. V., BEUKES, J. P., GALY-LACAUX, C., RAMANDH, A. & PIENAAR, J. J. 2020c. Measurement report: Statistical modelling of long-term trends of atmospheric inorganic gaseous species within proximity of the pollution hotspot in South Africa. 20.
TANAKA, P. L., OLDFIELD, S., NEECE, J. D., MULLINS, C. B. & ALLEN, D. T. 2000. Anthropogenic Sources of Chlorine and Ozone Formation in Urban Atmospheres. *Environmental Science & Technology,* 34**,** 4470-4473.
TELEDYNE API 2019. User Manual Models T200 and T200U NO/NO2/NOX Analyzers.
THERMO FISHER SCIENTIFIC 2007a. Model 43i Instruction Manual Pulsed Fluorescence SO2 Analyzer.
THERMO FISHER SCIENTIFIC 2007b. Model 49i Instruction Manual UV Photometric O3 Analyzer.
TIITTA, P., VAKKARI, V., CROTEAU, P., BEUKES, J. P., VAN ZYL, P. G., JOSIPOVIC, M., VENTER, A. D., JAARS, K., PIENAAR, J. J., NG, N. L., CANAGARATNA, M. R., JAYNE, J. T., KERMINEN, V. M., KOKKOLA, H., KULMALA, M., LAAKSONEN, A., WORSNOP, D. R. & LAAKSO, L. 2014. Chemical composition, main sources and temporal variability of PM₁ aerosols in southern African grassland. *Atmos. Chem. Phys.,* 14**,** 1909-1927.

TÖRÖK, B. L. & DRANSFIELD, T. 2018. Green chemistry : an inclusive approach. Amsterdam, Netherlands: Elsevier.

ÜZMEZ, Ö. Ö. 2018. Atmospheric concentrations of inorganic pollutants (NO2, SO2 and ozone) in Eskişehir: spatial and vertical variations, weekday-weekend differences. *Anadolu University Journal of Science and Technology A-Applied Sciences and Engineering,* 19**,** 523-535.

VAKKARI, V., TIITTA, P., JAARS, K., CROTEAU, P., BEUKES, J. P., JOSIPOVIC, M., KERMINEN, V. M., KULMALA, M., VENTER, A. D. & VAN ZYL, P. G. 2015. Reevaluating the contribution of sulfuric acid and the origin of organic compounds in atmospheric nanoparticle growth. *Geophysical Research Letters,* 42**,** 10,486-10,493.

VARDOULAKIS, S., LUMBRERAS, J. & SOLAZZO, E. 2009. Comparative evaluation of nitrogen oxides and ozone passive diffusion tubes for exposure studies. *Atmospheric Environment,* 43**,** 2509-2517.

VELYCHKO, O. & GORDIYENKO, T. Evaluation of the long-term drift of measuring instruments and standards using time series. 26 th IMEKO TC4 International Symposium and 24 th International Workshop on ADC/DAC Modelling and Testing, 2023. 1-5.

WALDMAN, J., MUNGER, J. W. & JACOB, D. J. 1992. *Measurement methods for atmospheric acidity and acid deposition*, Elsevier, London.

WANG, Y., ALI, M. A., BILAL, M., QIU, Z., MHAWISH, A., ALMAZROUI, M., SHAHID, S., ISLAM, M. N., ZHANG, Y. & HAQUE, M. N. 2021. Identification of NO2 and SO2 Pollution Hotspots and Sources in Jiangsu Province of China. *Remote Sensing,* 13**,** 3742.

WICKHAM, H. 2016. *ggplot2: Elegant Graphics for Data Analysis,* New York, Springer-Verlag.

WICKHAM, H. A., M. BRYAN, J. CHANG, W. MCGOWAN, L. D. FRANÇOIS, R. GROLEMUND, G. HAYES, A. HENRY, L. HESTER, J. KUHN, M. PEDERSEN, T. L. MILLER, E. BACHE, S. M. MÜLLER, K. OOMS, J. ROBINSON, D. SEIDEL, D. P. SPINU, V. TAKAHASHI, K. VAUGHAN, D. WILKE, C. WOO, K. YUTANI, H. 2019. {Welcome to the {tidyverse}. *Journal of Open Source Software,* 4**,** 1686.

ZBIERANOWSKI, A. & AHERNE, J. 2012. Ambient concentrations of atmospheric ammonia, nitrogen dioxide and nitric acid across a rural–urban–agricultural transect in southern Ontario, Canada. *Atmospheric Environment,* 62**,** 481–491.

ZHENG, C., ZHAO, C., LI, Y., WU, X., ZHANG, K., GAO, J., QIAO, Q., REN, Y., ZHANG, X. & CHAI, F. 2018. Spatial and temporal distribution of NO2 and SO2 in Inner Mongolia urban agglomeration obtained from satellite remote sensing and ground observations. *Atmospheric Environment,* 188**,** 50-59.